



HAL
open science

Long-term hydrolytic degradation study of polycaprolactone films and fibers grafted with poly(sodium styrene sulfonate): Mechanism study and cell response

Amélie Leroux, Tuan Ngoc Nguyen, André Rangel, Isabelle Cacciapuoti, Delphine Duprez, David G Castner, Veronique Migonney

► To cite this version:

Amélie Leroux, Tuan Ngoc Nguyen, André Rangel, Isabelle Cacciapuoti, Delphine Duprez, et al.. Long-term hydrolytic degradation study of polycaprolactone films and fibers grafted with poly(sodium styrene sulfonate): Mechanism study and cell response. *Biointerphases*, 2020, 15, 10.1116/6.0000429 . hal-03011219

HAL Id: hal-03011219

<https://hal.science/hal-03011219v1>

Submitted on 18 Nov 2020

HAL is a multi-disciplinary open access archive for the deposit and dissemination of scientific research documents, whether they are published or not. The documents may come from teaching and research institutions in France or abroad, or from public or private research centers.

L'archive ouverte pluridisciplinaire **HAL**, est destinée au dépôt et à la diffusion de documents scientifiques de niveau recherche, publiés ou non, émanant des établissements d'enseignement et de recherche français ou étrangers, des laboratoires publics ou privés.

This is the author's peer reviewed, accepted manuscript. However, the online version of record will be different from this version once it has been copyedited and typeset.
PLEASE CITE THIS ARTICLE AS DOI: 10.1116/6.0000429

1 Long-term Hydrolytic Degradation Study of Polycaprolactone Films and Fibers
2 Grafted with Poly(sodium styrene sulfonate) : Mechanism Study and Cell Response

3

4 Amélie Leroux, Tuan Nguyen, André Rangel, Isabelle Cacciapuoti, Delphine Duprez, David G.
5 Castner, Véronique Migonney*

6

7

8 Prof. Véronique Migonney, Dr. Amélie Leroux, Dr. André Rangel and Tuan Nguyen: Laboratory of
9 Biomaterials and Polymers of Specialty, CSPBAT UMR CNRS 7244 , Institut Galilée, Université
10 Sorbonne Paris Nord, Villetaneuse, France, E-mail : veronique.migonney@univ-paris13.fr

11 Isabelle Cacciapuoti : Inovarion, Paris, France

12

13 Dr. Delphine Duprez: Sorbonne Université, Institut Biologie Paris Seine, CNRS, UMR 7622,
14 Laboratoire de Biologie du Développement, INSERM U1156, F75005 Paris, France

15

16 Prof. David G. Castner: National ESCA and Surface Analysis Center for Biomedical Problems
17 (NESAC/Bio), Departments of Bioengineering and Chemical Engineering, University of
18 Washington, Box 351653, Seattle, WA, USA

19

20

21

22 **Keywords**

23 polycaprolactone, degradation, bioactive functionalization, biomaterials, tissue engineering

24 **Abstract**

25 Polycaprolactone (PCL) is a widely used biodegradable polyester for tissue engineering applications when
26 long-term degradation is preferred. In this article, we focused on the analysis of the hydrolytic degradation of
27 virgin and bioactive poly(sodium styrene sulfonate) (pNaSS) functionalized PCL surfaces under simulated
28 physiological conditions (phosphate buffer saline at 25°C and 37°C) for up to 120 weeks with the aim of
29 applying bioactive PCL for ligament tissue engineering. Techniques used to characterize the bulk and surface
30 degradation indicated that PCL was hydrolyzed by a bulk degradation mode with an accelerated degradation -
31 three times increased rate constant - for pNaSS grafted PCL at 37°C when compared to virgin PCL at 25°C.
32 The observed degradation mechanism is due to the pNaSS grafting process (oxidation, radical polymerization)
33 which accelerated the degradation until 48 weeks, when a steady state is reached. The PCL surface was altered
34 by the pNaSS grafting, introducing hydrophilic sulfonate groups that increase the swelling and smoothing of
35 the surface, which facilitated the degradation. After 48 weeks, pNaSS was largely removed from surface and
36 the degradation of virgin and pNaSS grafted surfaces were similar. The cell response of primary fibroblast
37 cells from sheep ligament were consistent with the surface analysis results: a better initial spreading of cells
38 on pNaSS surfaces when compared to virgin surfaces and a tendency to become similar with degradation time.
39 It is worthy to note that during the extended degradation process the surfaces were able to continue inducing
40 better cell spreading plus preserve their cell phenotype as shown by collagen genes expressions.

41

42 **1. Introduction**

43 Polycaprolactone (PCL) and its copolymers are used in a large number of medical devices and in
44 tissue engineering. The slow degradation rate of PCL allows it to stay several months *in vivo* without
45 significant degradation.^[1,2] Plus, these polymers have many advantages such as (i) flexible
46 mechanical properties; ^[3,4,5] (ii) ease of processing and fabrication; ^[6,7,8] (iii) adjustable degradation
47 kinetics by varying crystallinity, molecular weight, structure geometry (porosity, thickness,
48 etc.);^[9,10,11] and (iv) the possibility of being functionalized.^[12, 13] Currently, there are two common

49 approaches to modifying materials to improve their biocompatibility: surface coating or chemical
50 modification/functionalization of the surface. Functionalization of the surface is generally done by
51 the coupling of small molecules via covalent, ionic or hydrophobic interactions. ^[14,15] On the other
52 hand, surface coating can be done by depositing the molecule of interest via methods such as plasma
53 spraying, thermal spraying or electrolytic deposition. ^[16,17] For hydrophobic polyesters like PCL these
54 strategies are of particular interest for making their surface more cell adherent and biocompatible
55 to induce favorable interactions with proteins and cells.

56 For several decades our laboratory has successfully developed functionalization methods of polymer
57 surfaces introducing carboxylate and/or sulfonate groups for mimicking glycoaminoglycans
58 functionality and improving cell interaction to improve bio-integration of medical devices. ^[18,19,20]
59 Especially, the development of grafting poly(sodium styrene sulfonate) (pNaSS) on polyethylene
60 terephthalate (PET) LARS[™] ligaments led to a new generation of biointegrable and bioactive
61 synthetic ligaments. ^[21,22,23] The excellent *in vitro* and *in vivo* results in a large animal model (i.e.,
62 sheep) demonstrated that the pNaSS grafting provided (i) an increase of the cell adhesion strength;
63 ^[22] (ii) a better morphology of the cells that were more spread out and more homogeneously
64 distributed; ^[23,24,25] (iii) an increase of the type-I collagen production that was accompanied by tissue
65 formation with a better organization; ^[24,26] (iv) an improved osteointegration of the prosthesis with
66 the generation of a good bone-implant interface. ^[27] Based on that, the idea to develop the next
67 generation of synthetic ligament which could be biointegrable, bioactive and biodegradable emerged.
68 Thus, the pNaSS grafting was extended to PCL surfaces – films, scaffold, and fibers so far - and
69 bioactivity improvements of those modified materials were studied. ^[28, 29, 30] For the ligament
70 reconstruction application, the impact of the grafting process on mechanical properties as well as the
71 feasibility of a rat implantation model have been assessed and described. ^[31,32] The first studies on cell
72 response to pNaSS grafted PCL are encouraging, however, one essential question remains for the
73 ligament application: how long does the pNaSS-PCL ligament stay in the body before degrading and
74 are the mechanical properties and bioactivity maintained ?

75 In general, the degradation of poly(α -hydroxy esters) is stimulated by the specific action of water and
76 the phenomena of diffusion and reactions that occur within the material. Two distinct processes are
77 observed: (i) a surface degradation where the diffusion of water in the polymer volume is extremely
78 slow compared to the hydrolytic cleavage reaction; and (ii) a mass degradation where the water is
79 able to penetrate through the entire polymer so that random hydrolytic chain splits take place
80 uniformly throughout the matrix.^[33] As a poly(α -hydroxy ester), the degradation of PCL is carried
81 out by hydrolysis: the PCL chains are cleaved at the ester bonds, forming carboxyl terminal groups
82 and thereby reducing the size of the molecular chains and yielding water-soluble degradation products
83 such as 6-hydroxylcaproic acid.^[11,33, 34,35] When the by-products diffuse into the medium, the
84 degradation, and therefore the decrease of the molecular weight throughout the sample are
85 homogeneous, creating a balance between diffusion and hydrolysis reactions.^[36] In the case where
86 the by-products do not diffuse into the medium and remain trapped in the mass of the polymer, the
87 presence of the carboxylic acids will catalyze the hydrolysis. Under these conditions a concentration
88 gradient would be present in the material, with the rate of degradation of the core of the structure
89 occurring at an exponential rate due to internal autocatalysis.^[33]

90 Many research studies focus on the hydrolytic or enzymatic *in vitro* degradation of PCL copolymers,
91 usually containing polylactic acid, for short- to mid-term applications that are often less than one
92 year.^[37,38,39,40] Some other studies use accelerated degradation conditions such as extreme pH or UV
93 irradiation.^[41,42] Predictable mathematic models have also been developed specifically for polyester
94 degradation.^[43,44] Nevertheless, very few articles focused on the long-term (i.e., >1 year) hydrolytic
95 degradation of pure PCL in a saline solution at pH 7.4 and 37°C.^[45] Moreover, although the
96 degradation of some coated-PCL surfaces can be found in the literature,^[46,47,48,49] few studies
97 investigated the degradation of functionalized-PCL surfaces.^[50,51] This article has two main
98 objectives: (i) investigate the long-term hydrolytic degradation study of two PCL structures - films
99 with a spherulite structure and fibers bundles with a shish-kebab structure – at two degradation
100 temperatures (25°C and 37°C) in saline solution; and (ii) evaluate the impact of functionalization by

101 radical grafting on PCL degradation to investigate the mechanism of degradation for pNaSS-grafted
102 PCL samples. Therefore, the work presented here is organized in three parts: (i) the degradation study
103 to examine what is the mechanism of the hydrolytic degradation of pNaSS grafted PCL and how does
104 pNaSS impact the degradation reaction; (ii) the surface analysis of the degraded material; and (iii)
105 the biologic behavior of the resulting degraded structures.

106 **2. Materials and methods**

107 **2.1 Sample preparation**

108 *2.1.1 PCL film spin-coating*

109 PCL films were cast using a spin-coating method. Raw PCL pellets from Sigma-Aldrich (St Quentin
110 Fallavier, France) (sku. 704105, i.e. PC60 Mn = 60,000 g.mol⁻¹) were dissolved in dichloromethane
111 solution (30%, w/v) spin-coated for 30 sec at 1,500 rpm using a SPIN150-v3 SPS. The cast films
112 were then dried overnight at air pressure and room temperature. Using a punch, the cast films were
113 cut into 14-mm diameter disks and placed at 4°C until further experiments.

114 *2.1.2 PCL fiber bundles*

115 20 PCL fibers (diameter 110 ± 15µm) from Luxilon Industries, Belgium, were placed in a handmade
116 Teflon plate in which longitudinal and vertical grooves had been dug. The fibers were placed in the
117 vertical grooves and a PCL solution (1.2 g of PC60 dissolved in 2 ml of dichloromethane) was cast
118 in the longitudinal grooves. After overnight evaporation of the dichloromethane the 20 fibers were
119 joined together forming PCL fiber bundles with a nominal length of 30 ± 1 mm.

120 *2.1.3 Grafting of poly(sodium styrene sulfonate) (pNaSS) on PCL samples*

121 *Purification of the NaSS monomer*

122 Sodium 4-vinylbenzenesulfonate salt (sku. 94904, Sigma-Aldrich) was purified by recrystallization
123 in a mixed solution of ethanol-distilled water (90:10, v:v). Typically, 90 g NaSS were dissolved in
124 1,780 mL of the mixed solvent at 70°C overnight. The mixture was then filtrated and the filtrate

125 placed at 4°C for 48 h. After final filtration, the filter cake (recrystallized NaSS) was collected,
126 vacuum-dried for 6 h at 30°C, and kept at 4°C until further experiments.

127 *Radical grafting*

128 The PCL films and bundles were functionalized with pNaSS using a grafting "from" technique. 6 PCL
129 samples were placed in 100 mL of distilled water and ozonated either for 20 min (films) or 10 min
130 (bundles) at 30°C under stirring. Ozone was generated using an ozone generator BMT 802 N (ACW)
131 with a gas pressure of 0.5 bars and an oxygen flow rate of 0.6 L.min⁻¹. Next, the ozonated PCL
132 samples were transferred into a degassed aqueous NaSS solution (15%, w/v) under argon and
133 maintained for 3 h at 45°C under stirring to allow for radical polymerization of the monomer. The
134 grafted samples were extensively washed with distilled water for 48 h and then vacuum-dried.

135 **2.2 Degradation study design**

136 The degradation of PCL was assessed by immersion in a saline solution (0.5 ± 0.1 mg.mL⁻¹) at 25°C
137 or 37°C for 2.5 years in a controlled temperature chamber, without light exposure. The buffered saline
138 solution was composed of 0.14 mol.L⁻¹ NaCl, 0.01 mol.L⁻¹ Na₂HPO₄, 0.002 mol.L⁻¹ KH₂PO₄ and
139 0.05% of NaN₃ to avoid contamination. This solution was renewed every three months and its pH
140 was measured until the degradation time points were reached (original pH = 7.4). The degradation of
141 grafted and non-grafted PCL samples was evaluated at 0, 2, 4, 12 and 24 weeks and every 24 weeks
142 after that until 120 weeks (2.5 years).

143 *2.2.1 Characterization of degradation evolution*

144 *pH measurements*

145 At each time point and for each condition examined the solutions from three randomly assigned
146 samples were kept apart and the others were pooled together. The pH of those four solutions was
147 measured by a benchtop pH-meter (HI 2210, Hanna Instruments, France).

148 *Determination of molecular weights*

149 The PCL number average molecular weight (Mn), weight average molecular weight (Mw), and
150 polydispersity index (PDI) were determined by size exclusion chromatography (SEC) analysis using
151 a Shimadzu Prominence instrument LC20AD pump equipped with a SIL-20AHT auto sampler and
152 a Shimadzu RID-10A differential refractive index detector (Shimadzu Europa GmbH, Duisburg,
153 Germany). The PCL films and fibers were dissolved in tetrahydrofuran (ROTISOLV CLHP, Roth
154 Sochiel EURL, Lauterbourg, France) at 5 mg.mL⁻¹. The solutions were filtered (45µm) and eluted
155 through 2 SEC columns (phenomenex phenogel, Torrance, USA). A conventional calibration curve
156 was generated using a series of narrow polydispersity poly(methyl methacrylate) standards. Three
157 films or fibers samples were analyzed per condition.

158 *Differential scanning calorimetry method*

159 Differential scanning calorimetry (DSC) analyses were carried out with a DSC 8000 calorimeter
160 (Perkin Elmer, Waltham, USA) under nitrogen atmosphere. The samples were scanned once from
161 -75°C to 100°C at a heating rate of 10°C.min⁻¹. The glass transition temperature (T_g), melting
162 temperature (T_m), and melting enthalpy (ΔH_m) of the PCL films were determined from the first scan.
163 The glass transition temperature was assessed using the midpoint method (temperature at which the
164 measured curve is equidistant between the upper and lower tangents). The melting temperature was
165 taken at the maximum of the peak. The melting enthalpy was calculated as the melting peak area. The
166 degree of crystallinity (X_c) was calculated according to **Equation 1**:

167
$$X_c = \Delta H_m / \Delta H_{m0} \times 100$$

168 Where ΔH_{m0} stands for the melting enthalpy of 100% crystalline PCL (ΔH_{m0} = 135.44 J.g⁻¹).^[52]169 *Mechanical testing*

170 Mechanical assays were performed in a Bose Electroforce 3220 equipment (TA instruments, USA).
171 Only the PCL fibers bundles were examined. The effective length of samples was set at 10 mm and

172 the stain rate used was 3.6 mm.min⁻¹. Stress strain curves until rupture were recorded and Young's
173 Modulus E in MPa, elongation ε in % and the ultimate tensile stress (UTS) in MPa were determined.

174 *SEM images*

175 The micro-topography of PCL surface was carried out using a Hitachi TM3000 SEM operating at
176 15 kV. For PCL films, the two sides of the sample were observed. No specific sample preparation
177 was done.

178 *Atomic force microscope*

179 The nano-topography of the PCL surface was studied by Atomic force microscopy (AFM) using a
180 MultiMode 8 model (Bruker, Billerica, USA) and the NanoScope Analysis 1.8 software (Bruker).
181 Each PCL sample was analyzed in air at room temperature using the ScanAsyst mode (tapping mode).
182 The tip used was symmetric, 2.5 to 8 μm height with a spring constant of 0.4 N/m (70 Hz). The
183 cantilever was made from silicon nitride and had a triangular geometry. The regions of interest for
184 scanning were selected based on the view of the sample in the built-in optical microscope on the AFM
185 instrument. Scanning size performed on PCL was 500x500 nm².

186 Mean roughness was calculated by the **Equation 2**:

$$187 \quad Ra = \frac{1}{lr} \int_0^{lr} |Z(x)| dx, \text{ where Ra is arithmetic average (nm).}$$

188 *Contact angle measurements*

189 Static solvent contact angles were measured using a DSA10 contact angle measuring system from
190 KRUSS GmbH. A droplet of solvent was suspended from the tip of a microliter syringe supported
191 above the sample stage. The image of the droplet was captured and the contact angle was measured
192 using DSA drop shape analysis program from KRUSS-PT 100. The contact angle of dH₂O (2 μL) on
193 the surface was recorded 8s after contact, 3 measurements were taken and averaged.

194 The surface energy (γ_s) was calculated based on Young's equation:

$$195 \quad \gamma_s = \gamma_L \cos \theta + \gamma_{SL} \text{ (Equation 3)}$$

196 Where γ_L is the liquid surface free energy in $\text{mN}\cdot\text{m}^{-1}$; θ is the contact angle in $^\circ$; γ_{SL} is the solid/liquid
197 interfacial energy in $\text{mN}\cdot\text{m}^{-1}$.

198 The extended Fowker's method was used in these calculations: $\gamma_1 (1 + \cos\theta) = 2(\gamma_1^d \gamma_2^d)^{1/2} + 2 (\gamma_1^p$
199 $\gamma_2^p)^{1/2}$ (**Equation 4**)

200 Water (polar), ethylene glycol (polar) and methylene iodide (unpolar) were the liquids used.

201 *X-Ray photoelectron spectrometry (XPS) analysis*

202 All spectra were taken on a Surface Science Instruments S-probe spectrometer that has a
203 monochromatized Al $K\alpha$ X-ray and a low energy electron flood gun for charge neutralization of non-
204 conducting samples. The PCL film samples were fastened to the sample holder using double-sided
205 tape and run as insulators. X-ray spot size for these acquisitions was approximately 800 μm . Pressure
206 in the analytical chamber during spectral acquisition was less than 5×10^{-9} Torr. Pass energy for
207 survey spectra (to calculate composition) was 150 eV and pass energy for high resolution scans was
208 50 eV. The take-off angle (angle between the sample normal and the input axis of the energy analyzer)
209 was approximately 0° . This take-off angle corresponds to a sampling depth of approximately 100
210 \AA . The Service Physics Hawk Data Analysis Software was used to determine peak areas using a linear
211 background, to calculate the elemental compositions from peak areas, and to peak fit the high-
212 resolution spectra. The binding energy scales of the high-resolution spectra were calibrated by
213 assigning the lowest binding energy C1s high-resolution peak a binding energy of 285.0 eV. Three
214 spots were analyzed on each sample for determining the elemental composition. Analysis included a
215 survey spectrum, detailed spectra of the Na1s, N1s, S2p, and Si2p peaks, along with a high-resolution
216 spectrum of the C1s peak from one spot on each sample. Due to the geometry of fibers, this analysis
217 could not be performed on PCL bundles.

218 *Colorimetric method*

219 The evidence of the pNaSS grafting was tested using the toluidine blue colorimetric assay. The
220 method described by Ciobanu *et al* [21] was adapted as follows: an aqueous solution of toluidine blue

221 (Roth Sochiel EURL) was prepared at 5×10^{-4} M and drops of 1 M NaOH was slowly added to reach
222 and maintain the pH solution value of 10.0 ± 0.1 . Samples were immersed in 5 mL of this solution at
223 30°C for 6 h and then washed three times in 5 mL of 10^{-3} M NaOH for 5 min. Each sample was placed
224 in aqueous acetic acid solution (50%, v/v) - in 10 mL for films and in 2 mL for fibers - for 24 h at
225 room temperature. The decomplexation solution was analyzed by UV/visible spectroscopy (Perkin
226 Elmer lambda 25 spectrometer, Waltham, USA) at 633 nm. On the grafted surfaces, 1 mole of
227 toluidine blue was assumed to complex 1 mole of sulfonate group from pNaSS. The grafting rate
228 (GR) in mol.g^{-1} was then calculated according to **Equation 5**:

$$229 \quad GR = \frac{OD \cdot V}{\epsilon \cdot l \cdot m}$$

230 Where, OD is the optical density, V is the aqueous acetic acid volume (L), ϵ is the extinction
231 coefficient of toluidine blue solution ($\text{L.mol}^{-1}.\text{cm}^{-1}$), l is the length of the spectrophotometer tank
232 (cm), and m is the mass of the PCL films (g). The extinction coefficient was calculated based on a
233 dilution curve using the initial toluidine blue solution.

234 *ATR-FTIR analyses*

235 The Fourier-transformed infrared (FTIR) spectra, recorded in an attenuated total reflection (ATR),
236 were obtained using a Perkin Elmer Spectrum Two spectrometer. The PCL films were uniformly
237 pressed against a diamond crystal and for each surface, 128 scans were acquired from 4000 to 400
238 cm^{-1} at a resolution of 2 cm^{-1} .

239 *2.2.2 Cell culture analyses*

240 *Preparation of the samples for cell culture*

241 Prior to experiments, all PCL films were packaged and sterilized as follows: 3x washing (3 h in 0.15
242 M NaCl), 20 min in 70% ethanol, 10 min in ultra-pure water, and 15 min UV irradiation (both sides
243 of the samples). All steps were performed under stirring. The PCL films were kept in sterile PBS
244 solution at -20°C until further experiments. The samples were then slowly defrozen and placed
245 overnight at 37°C under 5% CO_2 in cell culture medium (DMEM, Gibco) without supplementation

246 followed by an overnight incubation at 37°C under 5% CO₂ in cell culture medium supplemented
247 with 10% FBS.

248 *Isolation and culture of primary sheep anterior cruciate ligament fibroblasts*

249 Anterior cruciate ligaments (ACL) were isolated from one sheep (2-year old female Merino sheep
250 free of degenerative joint disease, ~ 60 kg) in accordance with the German legislation on protection
251 of animals and the NIH Guidelines for the Care and Use of Laboratory Animals [NIH Publication 85-
252 23, Rev. 1985], and as approved by the local governmental animal care committee.^[53] Tissues were
253 cut into small pieces of 1-2 mm², washed three times in DPBS, and incubated in a 0.1% (w/v)
254 collagenase (Sigma-Aldrich) for 6 h at 37°C under 5% CO₂. The mixture solution was centrifuged 3
255 min at 1,500 rpm. The supernatant was withdrawn and the clot resuspended in DMEM complemented
256 with 10% bovine calf serum (BCS) (Sigma-Aldrich), 1% penicillin-streptomycin (Gibco), and 1% L-
257 glutamine (Gibco). The primary sheep ACL (sACL) fibroblasts were maintained in T-75 flasks until
258 confluence was reached. pNaSS-grafted and non-grafted PCL films were placed on the bottom of a
259 24-well plate using Teflon inserts. The cells were then seeded at a density of 5.10⁴ cells/well and
260 cultured at 37°C under 5% CO₂ over the time of the experiment.

261 *Cell viability*

262 PCL films were chemically degraded for one month in 2 mL of HCl solution (1 mol.L⁻¹) at 40°C. The
263 macroscopic degraded pieces of PCL were collected and analyzed by SEC; while, the solvent
264 suspensions were equilibrated to pH 7 with NaOH (1 mol.L⁻¹). After sterilization under 0.22 μm
265 filtration, the solutions containing the PCL degraded products were put in contact with sACL
266 fibroblasts for 24 h in DMEM complemented with 10% serum (dilution factor 1/5).

267 The medium was removed and 500 μL of MTT solution (Sigma, Saint Louis, USA) at final
268 concentration of 1 mg.mL⁻¹ diluted in fresh culture medium without phenol red was incubated for 4
269 h at 37°C. The supernatant was then discarded and 350 μL of DMSO was added to each well for 10
270 min at room temperature. Each well was thoroughly mixed and the absorbance was read at 570 nm.



This is the author's peer reviewed, accepted manuscript. However, the online version of record will be different from this version once it has been copyedited and typeset.
PLEASE CITE THIS ARTICLE AS DOI: 10.1116/6.0000429

271 The percentage of live cells in presence of PCL degraded products was calculated using a calibration
272 curve between the number of cells and the corresponding absorbance.

273 *Histological and fluorescence analyses*

274 sACL fibroblasts were harvested, fixed for 30 min with 4% formaldehyde, and rinsed twice with PBS.
275 For histological analyses (hematoxylin and eosin - H&E - staining), hematoxylin (Carl Roth GmbH,
276 Karlsruhe, Germany) was first added to each well for 10 min. The wells were then washed once with
277 distilled water and a solution of 1% HCl was briefly added. Prewarmed water (60°C) was added for
278 4 min, followed by addition of hematoxylin for 3 min, removal, and washing once with distilled water.
279 Eosin (Carl Roth GmbH) was then incubated for 2 min and extensively washed with distilled water.
280 Stained samples were kept at 4°C until observation under a light microscope (Olympus BX 45,
281 Hamburg, Germany).

282 For fluorescence analyses, the cells were fixed and the samples washed once with PBS and once with
283 3% bovine serum albumin (BSA)/PBS (Acros Organics, Geel, Belgium). The cells were then
284 permeabilized with 0.1% Triton-X 100 in PBS for 5 min at room temperature. After two washes in
285 PBS, the samples were incubated in 3% BSA/PBS for 1 h at room temperature. The cells were then
286 incubated with Fluorescein Phalloidin (FITC, Molecular probes, Eugene, USA) at 1:40 in 1%
287 BSA/PBS for 1 h at room temperature in the dark. After two washes in PBS, 2% 4',6-diamidino-2-
288 phenylindole (DAPI) dissolved in distilled water was added for 10 min at room temperature. The
289 samples were stored in distilled water at 4°C until observation under a fluorescent microscope
290 (Olympus CKX41).

291 *Total RNA extraction and real-time q-PCR analyses*

292 Sheep ACL cells were cultured for 7 days on grafted or non-grafted PCL films, which have been
293 subjected to 24, 48, 84 and 96 weeks of degradation. For each condition, total RNA was isolated
294 using the RNeasy mini kit according to the manufacturer's protocol (Qiagen, Hilden, Germany). For
295 each experimental condition, 100 ng RNA was reverse-transcribed using the high capacity
296 retrotranscription kit (Applied Biosystems, Thermo Fisher Scientific). Quantitative PCR was

This is the author's peer reviewed, accepted manuscript. However, the online version of record will be different from this version once it has been copyedited and typeset. PLEASE CITE THIS ARTICLE AS DOI: 10.1116/6.0000429

297 performed using SYBR Green PCR Master Mix (Applied Biosystems, Thermo Fisher Scientific)
 298 using the following primers (Sigma, Aldrich, Merck), COL1A1 (type-I collagen alpha 1), COL2A1
 299 (type-II collagen alpha 1), and COL3A1 (type-III collagen alpha 1), which are listed in Table 1.
 300 COL1A1 and COL3A1 identify ligament collagens, while COL2A1 identifies cartilage collagen. We
 301 used GAPDH as housekeeping gene for internal control. All primers were used at the 3 μ M final
 302 concentration. The threshold cycle (Ct) value for each gene of interest was measured for each
 303 amplified sample by using the StepOne software (Applied Biosystems, Thermo Fisher Scientific) and
 304 was normalized to GAPDH expression. The relative mRNA levels were calculated using the $2^{-\Delta\Delta Ct}$
 305 method described by Livak and Schmittgen.^[54] The ΔCt values were obtained by calculating the
 306 differences: Ct(gene of interest) – Ct(housekeeping gene) in each sample. We obtained the $\Delta\Delta Ct$
 307 values by calculating the differences between $\Delta Ct(\text{Experiment})$ and the average of $\Delta Ct(\text{control})$
 308 values. For relative mRNA level analysis, the COL2A1 values of non-grafted and non-degraded PCL
 309 were used as control and normalized to 1.

Table 1. Primers used for q-PCR

COL1A1	Forward	5'-
	CGTGATCTGCGACGAACTTA-3'	
	Reverse	5'-
	TCCAGGAAGTCCAGGTTGTC-3'	
COL2A1	Forward	5'-
	CAACCAGGACCAAAGGGACA-3'	
	Reverse	5'-
	GTCACCACGATCACCTCTGG-3'	
COL3A1	Forward	5'-
	CCGTGCCAAATATGCGTCTG-3'	
	Reverse	5'-
	GTGGGCAAACACTGCACAACAT-3'	
GAPDH	Forward	5'-
	ACAGTCAAGGCAGAGAACGG-3'	
	Reverse	5'-
	CCAGCATCACCCCACTTGAT-3'	

311

312 *Statistical analysis*

313 All the bulk analyses were carried out on three independent samples, all the surface analyses were
 314 carried out on three different spots on one sample, all the biologic experiments were carried out using



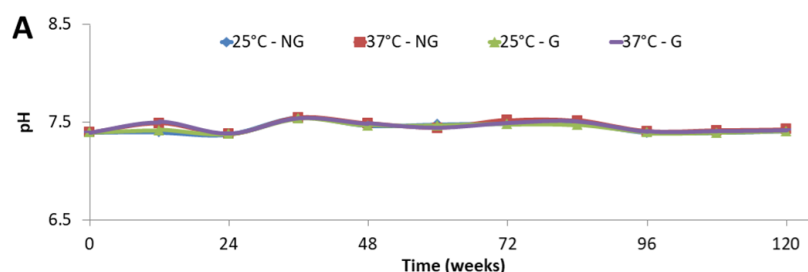
315 one to three samples per condition. Statistical analyses were performed using ANOVA with $p \leq 0.05$
316 considered statistically significant.

317 3. Results

318 3.1 Bulk analysis of degraded material

319 3.1.1 pH measurement

320 No significant change was found in the pH of the solution after 120-weeks of degradation ($p > 0.05$),
321 the pH never deviated more than 3% from the original 7.4 pH value for the different conditions studied
322 (see **Figure 1** for films and **Figure S1** in Supplementary Materials for fibers).



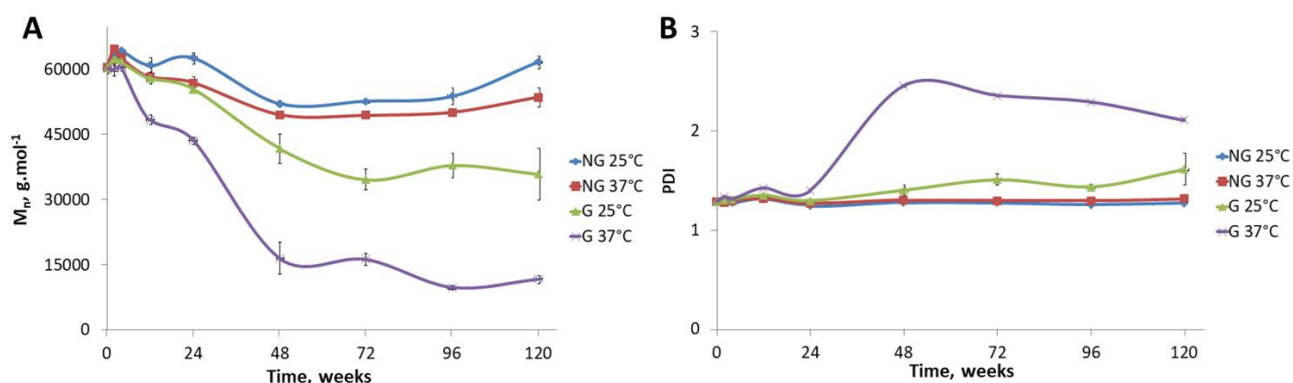
323 **Figure 1.** pH variation of the saline solution used for degradation of PCL films.
324

325 3.1.2 Molecular weight

326 The monitoring of the molecular weights over time revealed different degradation processes,
327 depending on the sample type and experimental conditions (cf. **Figure 2A**). For the non-grafted
328 samples M_n decreased slowly over the first year (i.e., 48 weeks) and then reached a plateau. After 2.5
329 years of degradation (i.e., 120 weeks), the non-grafted PCL film molecular weight decreased by 11.4
330 $\pm 2.6\%$ ($p \leq 0.05$). The PDI of the non-grafted films remained constant over the 2.5 years period with
331 a value of 1.29 ± 0.02 (cf. **Figure 2B**). These trends in M_n and PDI were similar whether the
332 degradation occurred at 25°C or 37°C , even if the loss in molecular weight was slightly increased at
333 the higher temperature ($p \leq 0.05$).
334

335 For the grafted samples, the degradation kinetics were significantly different ($p \leq 0.05$). First, the
336 molecular weight loss depended on the degradation temperature, 25°C or 37°C . At 25°C , the

337 molecular weight loss of the pNaSS grafted samples was $8.0 \pm 1.4\%$ ($p \leq 0.05$) after the first 6 months,
 338 increased to $30.7 \pm 6.2\%$ loss ($p \leq 0.05$) after 1 year and finally stabilized at $40.1 \pm 2.7\%$ loss ($p \leq$
 339 0.05) after 1.5 years (cf. **Figure 2A**). The PDI increased as M_n decreased, reaching a value of $1.49 \pm$
 340 0.10 ($p \leq 0.05$) after 1.5 years of degradation (cf. **Figure 2B**). Degradation of the pNaSS grafted
 341 sample was accelerated at 37°C compared to 25°C . After 6 months the molecular weight decrease
 342 was $27.7 \pm 0.2\%$ ($p \leq 0.05$) and reached a plateau at 1 year corresponding to $76.5 \pm 6.3\%$ of molecular
 343 weight loss ($p \leq 0.05$) (cf. **Figure 2A**). The PDI variation for this sample was different from the other
 344 conditions, for the first 6 months (i.e. 24 weeks) the PDI was stable at 1.35 ± 0.06 and then it increased
 345 to 2.30 ± 0.15 ($p \leq 0.05$) after 1 year of degradation (cf. **Figure 2B**).
 346 Similar trends, but to a lesser extent, were observed for degradation of the PCL bundles (cf. **Figure**
 347 **S2** in Supplementary Materials). The initial molecular weight of the fibers was higher than the films
 348 (i.e., $74,317 \pm 412 \text{ g.mol}^{-1}$ for the fibers *versus* $60,438 \pm 203 \text{ g.mol}^{-1}$ for the films), which slowed
 349 down the degradation process of the fiber bundles.



350
 351 **Figure 2.** SEC analysis results. (A) evolution of M_n over degradation time, (B) evolution of PDI over
 352 degradation time

353

354 3.1.3 DSC

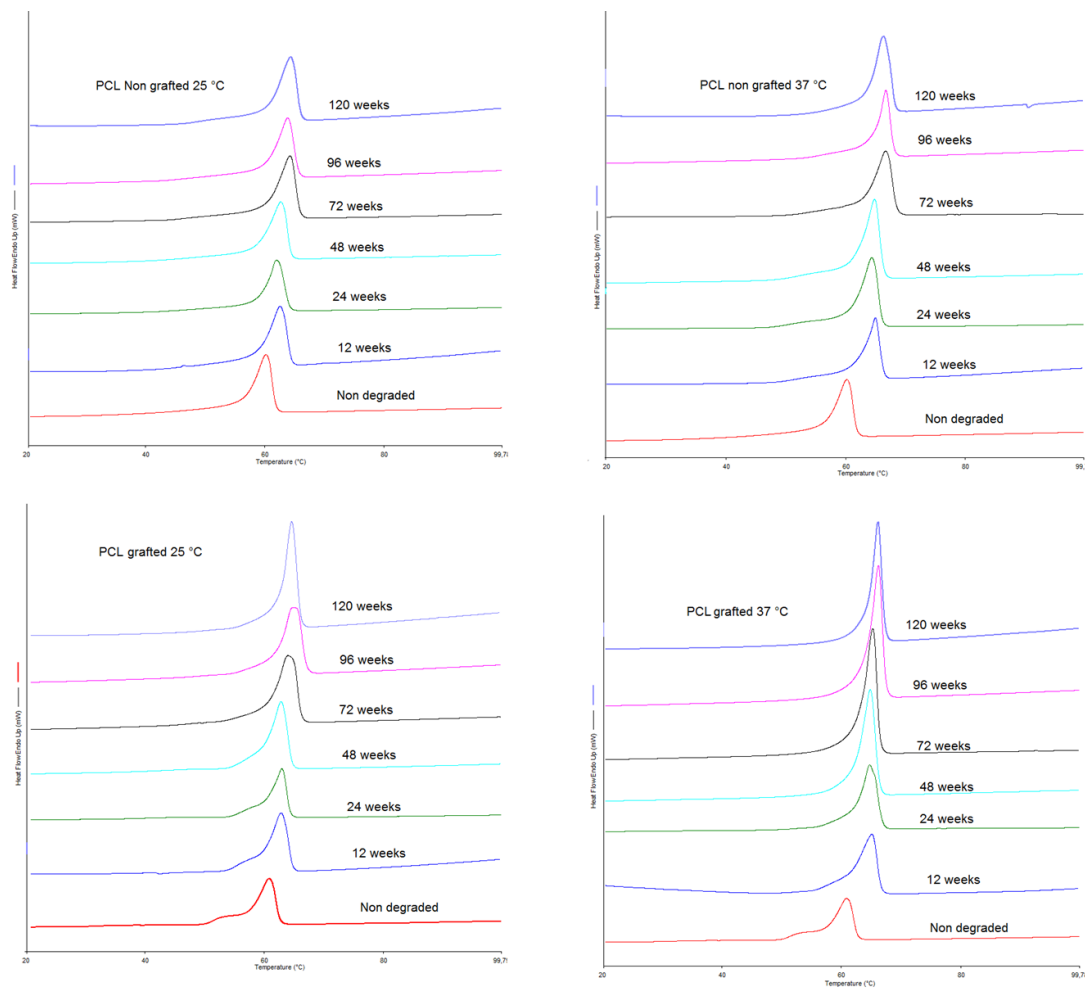
355 For all conditions, the degradation of the films was linked to increases in crystallinity and melting
 356 temperature (T_f). Although, it occurs differently at 25°C compared to 37°C .

357 The crystallinity of the non-grafted samples degraded at 25°C for 120 weeks increased by 4.4% ($p >$
 358 0.05), whereas the crystallinity of the grafted samples at 25°C for 120 weeks increased by 12.8% ($p >$

This is the author's peer reviewed, accepted manuscript. However, the online version of record will be different from this version once it has been copyedited and typeset.
PLEASE CITE THIS ARTICLE AS DOI: 10.1116/6.0000429

359 0.05). After 120 weeks at 37°C there was no difference between grafted and non-grafted samples,
360 which had crystallinity increases of 16.1% ($p \leq 0.05$). The increase of the crystallinity can be observed
361 by the size of the melting peak in the thermograms (**Figure 3**).

362 The degradation temperature significantly influenced the T_f , causing a shift in the melting peak. An
363 increase of 6% ($p \leq 0.005$) was observed when films were degraded at 25°C (from $T_f = 60.52 \pm$
364 0.58°C to $T_f = 64.41 \pm 0.02^\circ\text{C}$) compared to an increase of 8.8% ($p \leq 0.005$) when degraded at 37°C
365 (from $T_f = 60.52 \pm 0.58^\circ\text{C}$ to $T_f = 66.34 \pm 0.20^\circ\text{C}$) (see **Figure 3**).



366

367 **Figure 3.** DSC thermograms of the first heat for non-grafted and grafted PCL film degraded for 0,
368 12, 24, 48, 72, 96, 120 weeks degradation at 25°C and 37°C.

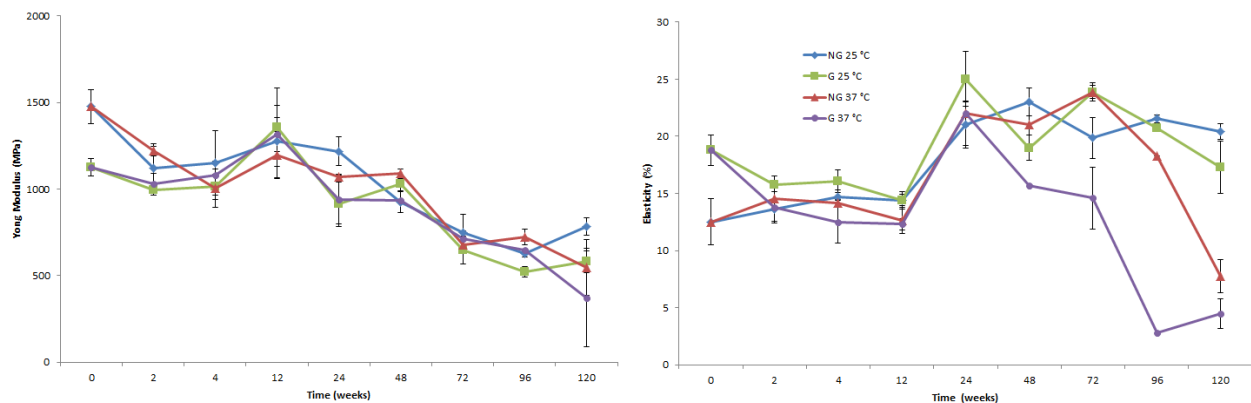
369



This is the author's peer reviewed, accepted manuscript. However, the online version of record will be different from this version once it has been copyedited and typeset. PLEASE CITE THIS ARTICLE AS DOI: 10.1116/6.0000429

370 3.1.4 Mechanical – fibers samples

371 Tensile tests were carried out over 2.5 years of degradation on the PCL bundles (20 fibers) to follow
 372 the evolution of crucial characteristics in the mechanical performance of the studied materials. After
 373 only 2 weeks of degradation, all samples exhibited a reduction of the Young Modulus values ($p >$
 374 0.05), the reduction being more prominent for non-grafted samples, which reached the same mean
 375 value of the grafted samples after 4 weeks of degradation (i.e., $E \approx 1075$ MPa) (cf. **Figure 4A**). Those
 376 values remained relatively stable for the next 20 weeks and then progressively decreased until 72
 377 weeks of degradation. From 72 to 120 weeks the Young modulus is once again relatively stable.
 378 Similarly, after the first two weeks of degradation the elastic strain for grafted and non-grafted
 379 samples converge to similar values (i.e., $\varepsilon \approx 14\%$, $p > 0.05$). These values remained relatively constant
 380 for the next 10 weeks and then experienced a substantial increase after 24 weeks of degradation ($p \leq$
 381 0.005). After 24 weeks the elastic strain of both samples degraded at 25°C remained fairly constant.
 382 In contrast the elastic strain of both samples degraded at 37°C decreased. The elastic strain decrease
 383 for the grafted sample began at 24 weeks and was more intense after 72 weeks, while for the non-
 384 grafted sample it didn't begin until 72 weeks (**Figure 4B**).

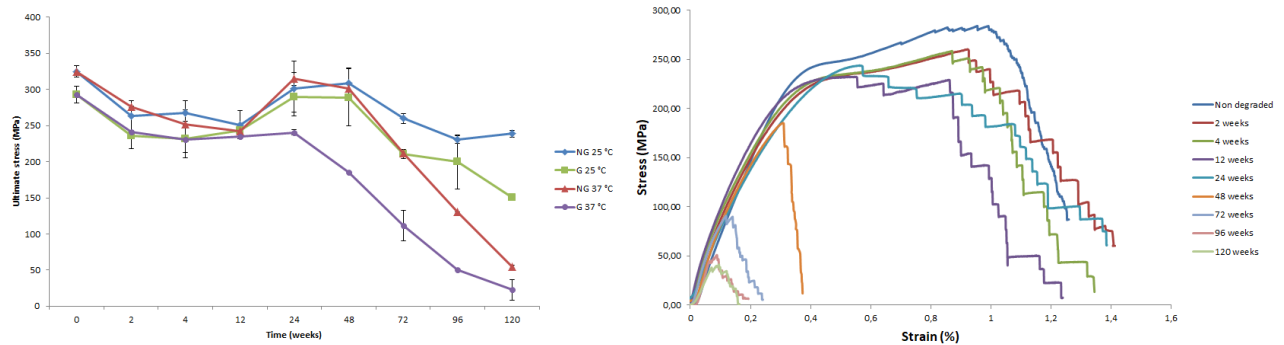


385 **Figure 4.** (A) Evolution of Young Modulus for PCL bundles over degradation time; (B) Evolution
 386 of elastic strain percentage for PCL bundles over degradation time.
 387

388
 389 The behavior of these two parameters can be associated with weakening of the material by the
 390 degradation process. The reduction of the ultimate stress also showed the grafted samples degraded
 391 more rapidly at 37°C ($p \leq 0.05$) (cf. **Figure 5A**). **Figure 5B** shows the stress-strain profiles for the

392 grafted sample degraded at 37°C along with the evolution of ultimate stress for all samples as a
393 function of degradation time.

394



395

396 **Figure 5.** (A) Evolution of the ultimate stress with degradation time; (B) Strain stress curves for
397 grafted samples degraded at 37 °C

398

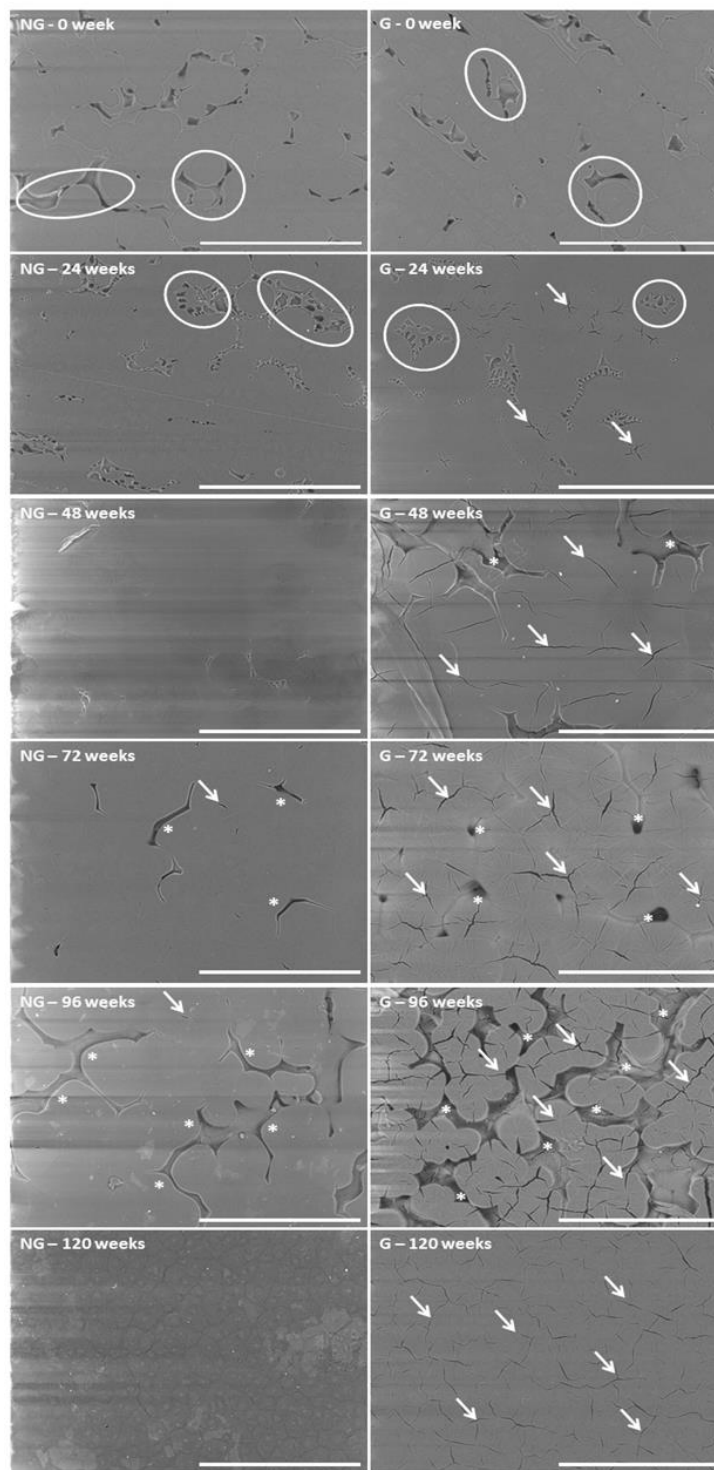
399 3.2. Surface analysis of degraded samples

400 3.2.1 Micro-topography

401 PCL spin-coated films presented a microstructure composed by amorphous and crystalline parts
402 arranged in spherulites structures (see **Figure 6**). The pNaSS grafting did not change the size of the
403 spherulites nor their proportion in the films, but some straight lines appeared. After 24-weeks of
404 degradation, the non-grafted samples lost their amorphous part (see circles in Figure 6) while the
405 grafted films started to present additional cracks in the crystalline part (see arrows in Figure 6). At
406 48- and 72-weeks of degradation, we observed a rearrangement of the structure with an increase in
407 spherulite size. The grafted films presented some microscopic holes between spherulites and a lot of
408 cracks localized in the germination points (see respectively stars and arrows in Figure 6). At 96-
409 weeks, the spherulites returned to their initial size. The first layer of the grafted films started to
410 disappear and films became very brittle. It was less obvious on the non-grafted samples where almost
411 no cracks of the crystalline part appeared over degradation time. At 120-weeks of degradation, the
412 films recovered a homogenous micro-topography which looks very crystalline with the grafted films
413 still presenting a lot of cracks in this crystalline structure (see arrows in Figure 6).

414 The same observations were made on non-grafted and grafted films when degraded at 25°C.

This is the author's peer reviewed, accepted manuscript. However, the online version of record will be different from this version once it has been copyedited and typeset.
 PLEASE CITE THIS ARTICLE AS DOI: 10.1116/6.0000429



415

416

417

418

419

420

421

422

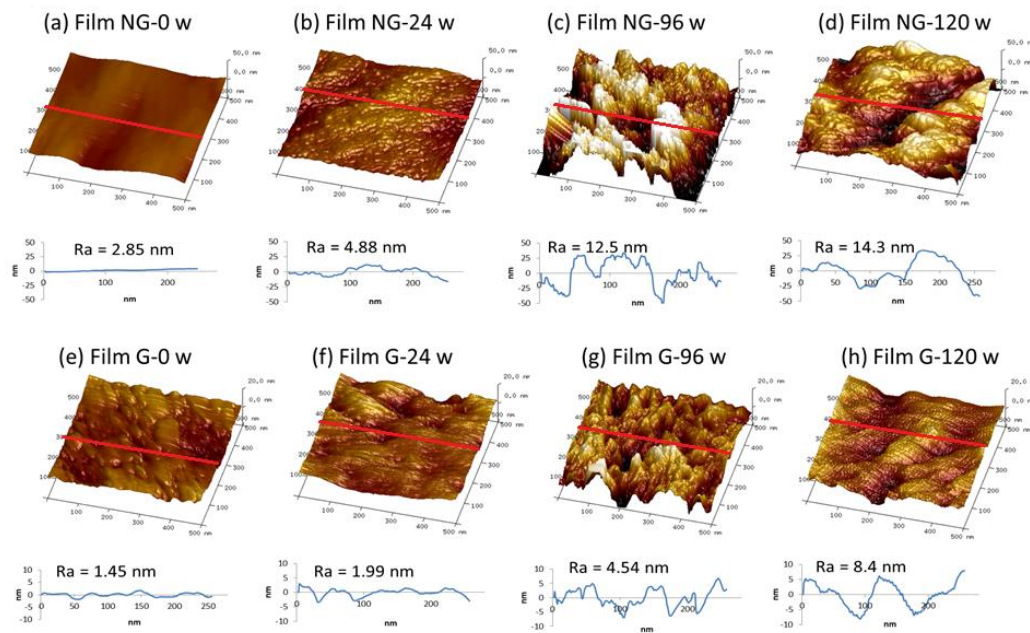
Figure 6. SEM images of non-grafted (NG) and pNaSS grafted (G) PCL films degraded at 37°C for 0-, 24-, 48-, 72-, 96- and 120 weeks. Scale bar = 300 μm. Legend: circle: amorphous part / arrow: cracks / star: hole

On PCL fibers bundles, due to spinning process, we assumed that the initial structure was organized in a shish-kebab pattern. The fibers micro-structure observed by SEM did not show any differences between non-grafted and grafted surfaces, or between 25°C- and 37°C- degradation. The only

423 observation was that fibers looked “rougher” (casting ridges accentuated) with degradation time and
 424 120-weeks of degradation at 37°C was required to start observing holes at the surface (see **Figure S3**
 425 in Supplementary Materials).

426 3.2.2 Nano-topography

427 AFM analysis demonstrated a difference in the surface topography between non-grafted and pNaSS
 428 grafted surfaces. The increase of image mean roughness (Ra) going from 2.85 nm at 0 weeks of
 429 degradation to 14.3 nm at 120 weeks of degradation ($p \leq 0.05$) demonstrated that the non-grafted
 430 surface became rougher after long term degradation. The degradation, represented by a roughness
 431 increase, also occurred with grafted film but was significant only after at 120 weeks of degradation
 432 (Ra = 8.4 nm, $p \leq 0.05$) (see **Figure 7**).



433 **Figure 7.** Nano-topography of non-grafted (NG) and grafted (G) PCL films degraded at 37°C: (a)
 434 Non-degraded NG film, (b) 24 w degraded NG film, (c) 96 w degraded NG film, (d) 120 w degraded
 435 NG film, (e) Non-degraded G film, (f) 24 w degraded G film, (g) 96 w degraded G film, (h) 120 w
 436 degraded G film. Scan size: 500×500 nm², the roughness diagram was measured over the red line.
 437

438
 439 The similar phenomenon happened with PCL fibers under the same conditions (see **Figure S4** in
 440 Supplementary Materials).



441 *3.2.3 Contact Angle measurement*

442 The non-grafted PCL films samples degraded at 25°C and 37°C, as well as the pNaSS grafted films
 443 degraded at 25°C, did not exhibit a significant change in their water contact angle measurements with
 444 degradation time ($p \leq 0.05$). In contrast, the pNaSS grafted films degraded over 120 weeks at 37°C
 445 displayed a significant decrease in the water contact angle going from 66.6 ± 0.9 to 54.0 ± 4.3 (28.1%
 446 decrease, $p \leq 0.05$). This decrease is consistent with an increase of the surface hydrophilicity with
 447 degradation (**Table 2**).

448 **Table 2.** Water contact angle on PCL film degraded over time at 25°C and 37°C.

Time (week)	Contact angle (°) water			
	Degradation at 25°C		Degradation at 37°C	
	Non grafted	Grafted	Non grafted	Grafted
0	77.0 ± 0.5	66.6 ± 0.9	77.0 ± 0.5	66.6 ± 0.9
12	77.4 ± 1.8	64.2 ± 5.1	68.3 ± 1.1	70.2 ± 3.6
24	77.9 ± 1.4	71.1 ± 3.0	76.0 ± 3.2	68.9 ± 0.6
48	76.5 ± 0.9	66.3 ± 6.9	72.3 ± 3.8	76.1 ± 2.6
72	71.3 ± 7.6	73.1 ± 4.8	82.1 ± 0.3	63.2 ± 0.6
96	71.4 ± 1.6	66.2 ± 0.2	75.4 ± 2.5	50.1 ± 3.1
120	72.8 ± 2.0	68.3 ± 2.3	73.0 ± 1.6	54.0 ± 4.3

449
 450 The surface energy, calculated according to **Equation 3** (see in Supplementary Materials Tables S1
 451 and S2 for contact angle results with ethylene glycol and diiodomethane), was higher on the grafted
 452 than on the non-grafted films due to the presence of sulfonate groups on the surface of the grafted
 453 films (see **Table 3**). The degradation of the PCL films did not significantly impact the surface energy
 454 ($p > 0.05$) and retained the initial difference observed between non-grafted and grafted samples.

455 **Table 3.** Surface energy (total) of non-grafted and grafted films degraded at 25°C and 37°C

Time (week)	γ_s (mN.m ⁻¹)			
	Degradation at 25°C		Degradation at 37°C	
	Non grafted	Grafted	Non grafted	Grafted
0	40.6 ± 0.3	44.5 ± 0.5	40.6 ± 0.3	44.5 ± 0.5
12	44.8 ± 1.1	46.0 ± 1.6	45.9 ± 0.9	46.9 ± 0.3
48	43.4 ± 0.4	45.9 ± 0.9	42.2 ± 1.4	43.9 ± 0.5
72	43.2 ± 0.5	46.4 ± 1.9	43.0 ± 0.3	46.0 ± 1.4
96	43.5 ± 1.6	45.6 ± 0.6	42.8 ± 0.7	52.4 ± 1.1
120	36.2 ± 2.6	47.0 ± 3.2	42.6 ± 0.9	53.2 ± 2.5

456 Additionally, the polar energy of non-grafted films was not changed by the degradation process, but
 457 an increase of this energy to $8.8 \pm 1.6 \text{ mN.m}^{-1}$ was observed for the grafted samples degraded at 37°C
 458 for 120-weeks (**table 4**).

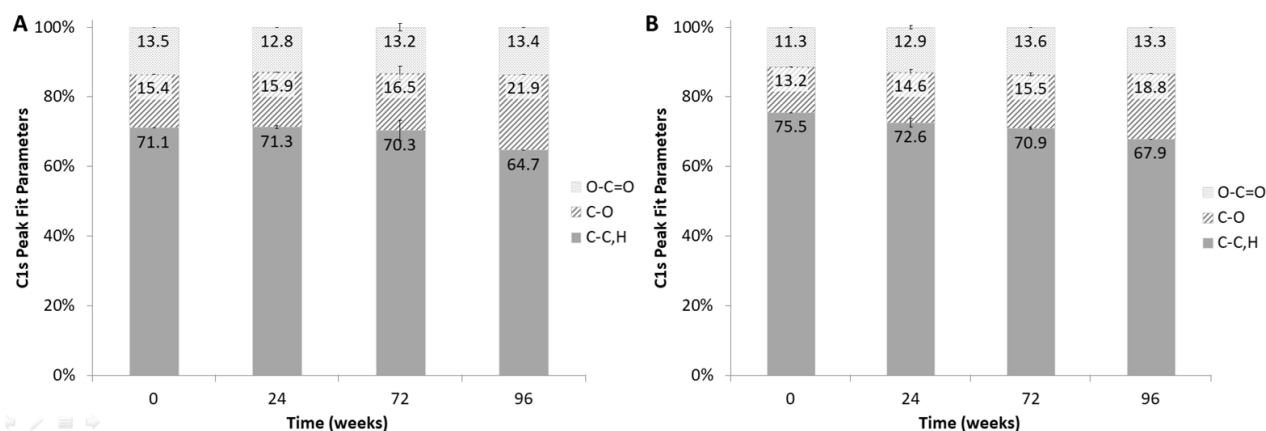
459 **Table 4.** Polar fraction of non-grafted and grafted films degraded at 25°C and 37°C

Time (week)	$\gamma^P \text{ (mN.m}^{-1}\text{)}$			
	Degradation at 25°C		Degradation at 37°C	
	Non grafted	Grafted	Non grafted	Grafted
0	2.4 ± 0.1	3.7 ± 0.2	2.4 ± 0.1	3.7 ± 0.2
12	1.6 ± 0.3	4.8 ± 0.5	4.1 ± 0.2	3.1 ± 0.3
48	2.1 ± 0.3	4.9 ± 0.6	2.8 ± 1.2	2.2 ± 0.4
72	2.7 ± 0.1	3.6 ± 1.3	1.0 ± 0.1	4.9 ± 0.5
96	3.5 ± 0.5	4.5 ± 0.2	3.3 ± 0.6	9.4 ± 0.9
120	2.8 ± 0.8	5.1 ± 1.1	3.7 ± 0.5	8.8 ± 1.6

460

461 3.2.4 XPS analysis

462 The XPS analysis provided information about the degradation of the PCL films in the outer $\sim 100 \text{ \AA}$
 463 of the samples. For the non-grafted samples degraded at 37°C , no significant variation of the carbon
 464 species concentrations was observed in the first 72 weeks of degradation, but at 96 weeks of
 465 degradation (i.e., 2 years) an increase of 42% of the C-O bonds was observed (cf. **Figure 8A**).
 466 Interestingly, the XPS analysis on the grafted PCL films presented the same increase of 42% in C-O
 467 bonds after 96 weeks of degradation, but with a more continual increase with degradation time (11%
 468 and 17% after 24 and 72 weeks of degradation, respectively) (cf. **Figure 8B**).



469



470

471

472

473

474

475

476

477

478

479

480

481

482

483

484

Figure 8. C1s peak fit parameters - percentages of atomic bonds for (A) non-grafted PCL films degraded overtime at 37°C and (B) grafted PCL films degraded overtime at 37°C.

The XPS determined atomic concentrations for all degraded PCL films were similar, but trace amounts of sulfur (~0.2 atomic percent) were detected on the grafted PCL films after degradation (see **Table 5**). The grafted samples prior to degradation exhibited a significantly different XPS elemental composition, due to the presence of the pNaSS film (increased sulfur, increased oxygen and decreased carbon). The colorimetric method could not be used to measure the amount of grafted pNaSS on the degraded samples due to a significant increase in the non-specific coloration of the degraded damaged surfaces ($p \leq 0.05$, see results on non-grafted samples in Table 5). XPS showed a decrease of the sulfur concentration (1.8 to 0.2 atomic percentage sulfur) upon degradation (see **Table 5**).

Table 5. Grafting rates (GR) determined according to equation 5 (see materials and methods) and surface concentration (XPS atomic percent) for non-grafted (NG) and grafted (G) PCL films degraded at 37°C for 0, 24, 72 or 96 weeks.

	GR ($\mu\text{mol.g}^{-1}$)		Atomic concentration %					
	before degradation	after degradation	C 1s	O 1s	S 2p	Na 1s	N 1s	Si 2p
NG – 0 week	0.70 \pm 0.27		72.1 \pm 0.9	22.7 \pm 0.9	-	-	-	3.4 \pm 0.1
NG – 24 weeks	1.05 \pm 0.45	0.99 \pm 0.35	76.3 \pm 0.4	21.9 \pm 0.4	-	0.2 \pm 0.1	-	1.7 \pm 0.2
NG – 72 weeks	0.47 \pm 0.40	2.13 \pm 0.70	76.8 \pm 0.9	20.2 \pm 0.9	0.1 \pm 0.0	0.3 \pm 0.1	1.5 \pm 0.6	1.1 \pm 0.3
NG – 96 weeks	0.30 \pm 0.12	7.26 \pm 0.96	73.1 \pm 0.8	22.7 \pm 0.7	0.1 \pm 0.1	0.6 \pm 0.1	2.3 \pm 0.2	1.2 \pm 0.1
G – 0 week	10.5 \pm 0.06		61.4 \pm 0.7	29.6 \pm 0.8	1.8 \pm 0.1	0.9 \pm 0.1	-	1.5 \pm 0.4
G – 24 weeks	8.51 \pm 0.81	41.30 \pm 5.46	74.5 \pm 0.0	22.5 \pm 0.4	0.3 \pm 0.0	0.6 \pm 0.0	-	2.2 \pm 0.4
G – 72 weeks	4.79 \pm 0.87	96.70 \pm 3.16	77.3 \pm 0.4	21.1 \pm 0.4	0.2 \pm 0.1	0.5 \pm 0.0	0.5 \pm 0.2	0.5 \pm 0.2
G – 96 weeks	3.31 \pm 1.34	156.00 \pm 9.57	75.5 \pm 0.9	22.9 \pm 0.9	0.2 \pm 0.0	0.7 \pm 0.1	0.4 \pm 0.2	0.3 \pm 0.1

485

486 3.2.5 Fourier Transforms Infrared Spectra

487

488

489

490

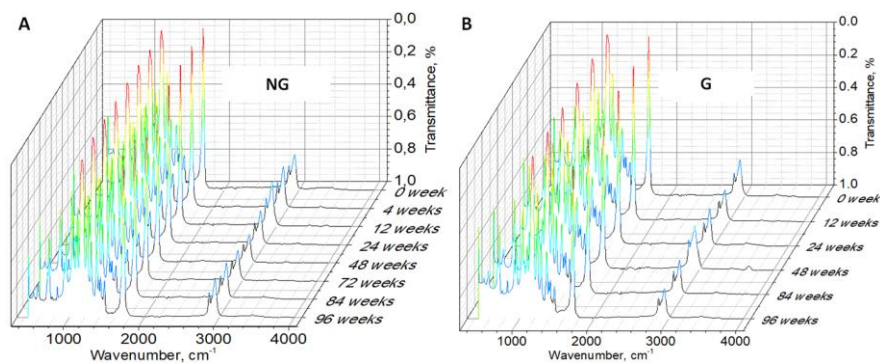
491

During the degradation process, the 1720 cm^{-1} ($\nu(\text{C}=\text{O})$) and 1167 cm^{-1} peaks ($\nu_{\text{as}}(\text{C}-\text{O})$) decreased (under 0.6 % of transmittance – see the decrease of red intensity on colors maps) after 84 weeks for the non-grafted PCL film (see **Figure 9**). The increase of a number of C-OH and COOH groups caused the significant decrease of these peaks. That phenomenon is related to the increased percentage of - CO bonds in the XPS C1s spectra as the degradation proceeded



This is the author's peer reviewed, accepted manuscript. However, the online version of record will be different from this version once it has been copyedited and typeset. PLEASE CITE THIS ARTICLE AS DOI: 10.1116/6.0000429

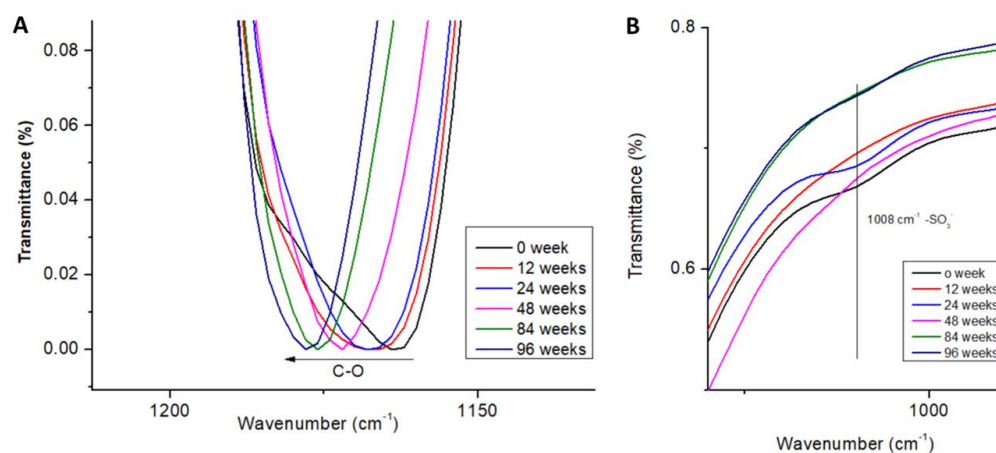
492



493

494 **Figure 9.** Fourier Transforms Infrared Spectra of non-grafted (A) and grafted (B) PCL films degraded
495 at 37°C over time.

496 The increase of alcohol and acid groups on polymer chain could be observed by a shift of the C-O
497 peak position.^[55] By breaking the C-O-C bond to form a C-OH bond, the C-O stretch changed, leading
498 to the blue-shift of the C-O peak from 1160 to 1180 cm⁻¹ (see **Figure 10A**). The decrease of
499 transmittance and the blue-shift of C-O peak are important keys to predict the surface degradation.
500 Following the sulfonate groups with degradation time, by monitoring the 1008 cm⁻¹ peak, revealed
501 the presence of sulfonate groups even after 96-weeks of degradation. However, this peak lost intensity
502 as the degradation process proceeded, as observed in the XPS analysis (see **Figure 10B**).



503

504 **Figure 10.** (A) The C-O-C peak of FTIR spectrum showing the blue shift with degradation time for
505 the grafted PCL samples degraded at 37°C and (B) evolution of -SO₃⁻ groups on grafted-PCL films
506 degraded at 37°C over time.

507 3.3 Impact on biologic behavior

508 3.3.1 Cell viability

509 A SEC analysis of the macroscopic pieces of PCL chemically degraded revealed a M_n of $11228 \pm$
510 2481 g.mol^{-1} independent of the grafting. This molecular weight was similar to that observed for
24

This is the author's peer reviewed, accepted manuscript. However, the online version of record will be different from this version once it has been copyedited and typeset.
PLEASE CITE THIS ARTICLE AS DOI: 10.1116/6.0000429

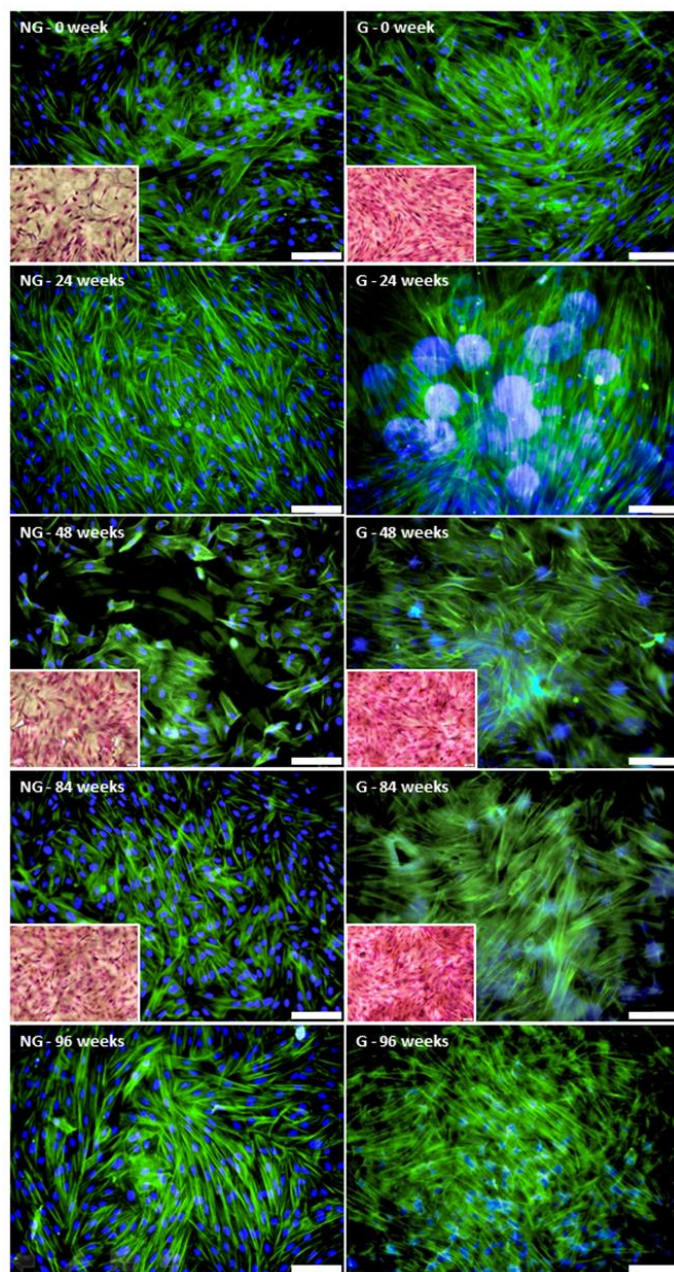
511 grafted-PCL films naturally degraded for 2.5-years at 37°C. The solution from the chemical
512 degradation was then put in contact to cells to study the cytotoxicity effect of the PCL degradation
513 products. The percentage of live cells in the degradation solutions from the non-grafted films and
514 grafted films was $100.01 \pm 0.12 \%$ and $100.26 \pm 0.22 \%$, respectively ($p > 0.05$).

515 3.3.2 Cell morphology

516 The fluorescence observations showed that primary ACL cells were better spread on the grafted PCL
517 films compared to the non-grafted PCL films (see **Figure 11**). Although the number of nuclei did not
518 seem to differ between the two conditions, the actin cytoskeleton was more developed for the cells
519 on the grafted samples. As the degradation of PCL proceeded at 37°C, the examination of the
520 fluorescence images became more complicated due to nonspecific attachment of the fluorochromes,
521 but it appeared the difference observed between the non-degraded non-grafted and grafted films was
522 maintained during the degradation process. These observations were confirmed with the
523 eosin/hematoxylin staining at selected time points. The same results were observed for the films
524 degraded at 25°C.

525

This is the author's peer reviewed, accepted manuscript. However, the online version of record will be different from this version once it has been copyedited and typeset.
PLEASE CITE THIS ARTICLE AS DOI: 10.1116/6.0000429



526

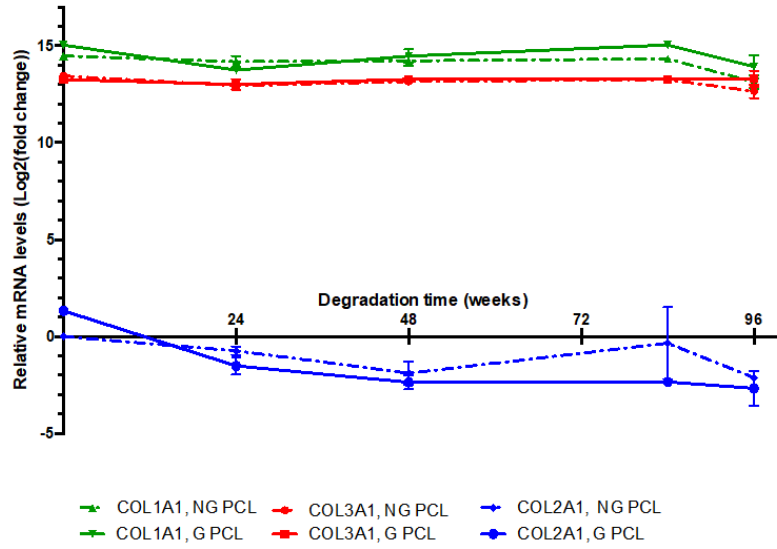
527

528 **Figure 11.** Morphologies of sACL fibroblasts seeded for 7 days on non-grafted (NG) and grafted (G)
529 PCL films degraded at 37°C over the time period shown. Phalloidin (green)/DAPI (blue) labelling
530 (scale bar = 100 μ m) and H&E staining (insets).

531 3.3.3 Gene expression

532 The expression of collagen genes, associated with the fibroblast/ligament phenotype, COL1A1 and
533 COL3A1, was not modified in sheep ACL cells cultured on grafted or non-grafted PCL films
534 subjected to degradation over the 96-week time period (see **Figure 12**). The expression of COL2A1
535 gene, a specific marker of cartilage, was not detected in sheep ACL cells at any of the experimental
536 conditions, indicating that ACL cells did not differentiate into cartilage when cultured on degraded

537 PCL. This molecular analysis showed that the PCL degradation process did not affect the ligament
538 phenotype of ACL cells.



539

540

541

542 **Figure 12.** RT-qPCR analysis of the expression levels of COL1A1, COL3A1 and COL2A1 genes in sheep ACL
543 cells, cultured during 7 days, on non-grafted (NG) and grafted (G) PCL films degraded at 37°C for 24, 48, 84 and
544 96 weeks. Graphs show means +/- standard deviations of 1 to 3 samples of gene expression. The relative mRNA
545 levels for each gene in the different experimental conditions were calculated as described in the Materials and
546 methods. For all genes and experimental conditions, the COL2A1 values of NG PCL at T=0 were used as control
547 and normalized to 1. Consequently, all the relative mRNA levels are comparable between them. Cts of COL2A1,
548 COL3A1 and COL1A1 were around 33 cycles, 20 cycles and 19 cycles, respectively. COL2A1 was not expressed
549 in the ACL cells, while COL3A1 and COL1A1 displayed high levels of expression in all the experimental
550 conditions.

551

552 4. Discussion

553 4.1 Bulk analysis of material degradation

554 The natural degradation of PCL samples – films and fibers bundles – with or without a grafted
555 bioactive polymer - was studied at two temperatures (i.e. 25°C and 37°C) for 120 weeks in a saline
556 solution. No change in the solution pH was observed, indicating that release of acid species from the
557 PCL degradation could not be detected.

558 The hydrolysis degradation process of the PCL polymeric chains appeared to be different when the
559 surface was grafted with pNaSS. In particular after six months the grafted samples exhibited
560 accelerated molecular weight losses and increased PDIs. It should be noted that during the first 6
561 months, the SEC determined molecular weights for 37°C-degraded grafted samples were only slightly
562 lower than the other samples and that the PDI results demonstrated that the PCL chains were cut
563 homogeneously during this time. After 6-months of degradation, the SEC results showed a drastic
564 drop of M_n and a significant increase of PDI. These effects were accentuated at the higher degradation
565 temperature. In all conditions, the degradation increased the global crystallinity of the polymer, as
566 determined by the increased melting temperature detected during the first scan of DSC for both films
567 and fibers bundles. This increase in crystallinity was due to the preferential loss of the amorphous
568 component in the films.

569 Although no significant M_n variation has been noticed, mechanical properties under rupture load on
570 non-grafted and pNaSS grafted PCL bundles reached the same level after 2 to 4 weeks of natural
571 degradation. This fact can be explained by two different phenomena: (i) the reduction of non-grafted
572 samples Young Modulus can be linked to the structure modification when in aqueous environment,
573 (ii) the temperature of the degradation media weakens the intermolecular bonds, reducing the required
574 tension to deform the fibers. ^[56] This decrease was less important for pNaSS grafted samples, since
575 the grafting process has already “thermally treated” the fibers. On the other hand, grafted samples
576 experienced a more severe increase of the crystallinity rate, which explains the more important
577 elasticity reduction on the early stages of degradation. In these first weeks an oscillation of UTS could

578 also be noticed. This behavior can be linked the combination of both of these phenomena and a
579 nonhomogeneous degradation of the fibers in the bundle. After this point, the studied properties (E ,
580 ε and σ_{\max}) remained relatively stable until 24 weeks of degradation and then became noticeably
581 modified by the degradation process (decreased E and σ_{\max} ; increased ε). In comparison to the native
582 human ligament, after 96 weeks of natural static degradation the grafted fibers had higher rigidity
583 (i.e., $E_{\text{PCL fibers, 96-weeks}} = 646 \pm 31 \text{ MPa}$ versus $E_{\text{native ligament}} = 114 \pm 53 \text{ MPa}$) and ultimate stress (i.e.,
584 $\sigma_{\max}(\text{PCL fibers, 96-weeks}) = 50.0 \pm 21.3 \text{ MPa}$ versus $\sigma_{\max}(\text{native ligament}) = 24.5 \pm 11.2 \text{ MPa}$). After 48 weeks
585 of natural static degradation the grafted fibers had higher elasticity (i.e. $\varepsilon_{\text{PCL fibers, 48-weeks}} = 15.7 \pm 1.4$
586 % versus $\varepsilon_{\text{native ligament}} = 12.0 \pm 4.2 \%$) than the native human ligament.

587 These bulk properties analyses demonstrated that even if the grafting accelerated the degradation
588 kinetics of the PCL samples, the physico-chemical and mechanical properties were sufficiently stable
589 for the 6 first months of natural degradation.

590 *4.2 Surface analysis with degradation*

591 The micro- and nano-topography observations were consistent with different modes of degradation
592 between the grafted and non-grafted samples. The degraded non-grafted films exhibited holes in the
593 amorphous regions, whereas the grafted films exhibited holes in the amorphous regions plus cracks
594 in crystalline regions. Moreover, at the nanoscale, the roughness increase of PCL surfaces after 120
595 weeks of degradation was lower on the grafted PCL films compared to non-grafted PCL films. These
596 observations suggest conservation of pNaSS grafting over degradation time.

597 The contact angle measurements showed an increase of 28% in the hydrophilicity of the grafted films
598 degraded at 37°C for 120 weeks, which can explain why the pNaSS grafting accelerated the
599 degradation process after 6 months. Furthermore, the polar energy also increased over time, consistent
600 with the surface segregation of polar groups linked to the PCL degradation.

601 Surface characterization demonstrated an increase of C-O species for all degradation conditions,
602 consistent with the hydrolysis of the ester bonds of the PCL. These results were consistent with the
603 degradation mechanism of the PCL described by Woodruff and Hutmacher.^[33] Noteworthy, the

This is the author's peer reviewed, accepted manuscript. However, the online version of record will be different from this version once it has been copyedited and typeset.
PLEASE CITE THIS ARTICLE AS DOI: 10.1116/6.0000429

604 molecular breakage was more gradual overtime on the pNaSS grafted surfaces compared to non-
605 grafted. In the XPS sampling depth - around 100Å depth - a decrease sulfur concentration over
606 degradation time was observed, but trace amounts of sulfur were still detected on all degraded, grafted
607 films. The colorimetric method commonly used to quantify the amount of sulfonate groups present
608 could not be used due to high levels on non-specific toluidine blue binding to the degraded polymer.
609 The surface characterization at a deeper sampling depths by FTIR demonstrated a reduction of the
610 C=O peak coupled with a blue shift of the C-O peak for all conditions over degradation time. These
611 results were relevant for the PCL degradation process, which consists of the cutting of the ester bonds
612 and was accelerated by the increase of degradation temperature as well as the pNaSS grafting. Finally,
613 the FTIR analysis, which probes deeper into the sample than XPS, detected the presence of pNaSS
614 after long-term degradation confirming the pNaSS grafting remains after long-term natural
615 degradation.

616 *4.3 Biological impact of degraded material*

617 The cytotoxicity experiments confirmed the absence of *in vitro* cytotoxicity from the PCL degradation
618 products, as has been reported in the literature,^[57] but also demonstrated no cytotoxicity from the
619 degradation products from the pNaSS grafted surface. The cell morphology study showed that cells
620 still have the ability to grow on the degraded surfaces, which likely was amplified by the increased
621 surface roughness produced by the degradation process.^[58,59] Moreover, it has been already
622 demonstrated that pNaSS grafting can modulate the fibroblast morphology, adhesion and
623 activity.^[22,27] With the morphology images presented in this article, we observed that the
624 improvement in cell spreading due to the pNaSS grafting still present for degradation times up almost
625 2 years. This result confirmed the effect of pNaSS and its presence over the long-term natural
626 degradation as observed by AFM, XPS, FTIR and contact angles. Finally, the collagen gene
627 expression revealed that primary ligament cells did not lose their phenotype when in contact with
628 degraded surface: they maintained a high and stable type-I and -III collagens gene expression without

629 significant differences between non-grafted and grafted surfaces. In contrast, the type-II collagen
630 gene, corresponding to the cartilage lineage, did not appear to be expressed in primary ligament cells.

631 **5. Conclusion**

632 This study evaluated the long-term hydrolytic degradation of two different types of PCL (films and
633 fibers) with different microstructures and molecular weights (i.e., films: $M_n = 60614 \pm 743 \text{ g.mol}^{-1}$
634 and spherulites structure *versus* fibers bundles: $M_n = 74674 \pm 2438 \text{ g.mol}^{-1}$ and shish kebab structure).

635 The obtained results confirmed the literature reports that PCL hydrolyzes by a bulk degradation mode
636 with increasing degradation kinetics for lower molecular weights and higher degradation
637 temperatures.^[11,36,60,61]

638 Nevertheless, the aim of this study was to evaluate the impact of the pNaSS grafting on the long-term
639 PCL degradation process. The obtained results showed a strong difference in the kinetics of the
640 degradation process. While PCL surfaces follows the extensively described process of PCL
641 degradation which depends on molecular weight, crystallinity and temperature^[33], in the case of the
642 pNaSS grafted samples the degradation still depends on the same parameters, but the presence of
643 grafted pNaSS macromolecular chains increases the hydrophilic properties of the PCL surfaces which
644 in turn strongly accelerates the surface degradation process. To address the question “would the
645 mechanical properties of pNaSS grafted PCL fibers be enough strong to act as a ligament prosthesis
646 after long term degradation?” the results from this study show the ultimate shear stress of the degraded
647 fibers after 96 weeks is higher than the ultimate shear stress of the natural ligament.

648

649

650 **Acknowledgments**

651 This work was funded as part of the "Future Investment Project" by the French Public Investment
652 Bank and the French state - PSPC application - Liga2bio project (VM). The XPS experiments done
653 at NESAC/Bio were supported by NIH grant EB-002027. We would like to thank Gerry Hammer



This is the author's peer reviewed, accepted manuscript. However, the online version of record will be different from this version once it has been copyedited and typeset.
PLEASE CITE THIS ARTICLE AS DOI: 10.1116/6.0000429

654 (NESAC/Bio) for his technical help with the XPS analysis and Laila Farias-Colaco for her technical
655 help on mechanical testing.

This is the author's peer reviewed, accepted manuscript. However, the online version of record will be different from this version once it has been copyedited and typeset.
PLEASE CITE THIS ARTICLE AS DOI: 10.1116/6.0000429

656 **References**

- 657 [1] H. Sun, L. Mei, C. Song, X. Cui, P. Wang, *Biomaterials* **27**, 1735 (2006).
- 658 [2] F. A. Petrigliano, G. A. Arom, A. N. Nazemi, M. G. Yeranorian, B. M. Wu, D. R. McAllister,
659 *Tissue Eng. Part A* **21**, 1228 (2015).
- 660 [3] C. P. Laurent, D. Durville, D. Mainard, J.-F. Ganghoffer, R. Rahouadj, *J. Mech. Behav. Biomed.*
661 *Mater.* **12**, 184 (2012).
- 662 [4] H. M. Pauly, D. J. Kelly, K. C. Popat, N. A. Trujillo, N. J. Dunn, H. O. McCarthy, T. L. H.
663 Donahue, “*J. Mech. Behav. Biomed. Mater.* **61**, 258 (2016).
- 664 [5] A. C. Gurlek, B. Sevinc, E. Bayrak, C. Erisken, *Mater. Sci. Eng. C* **71**, 820 (2017).
- 665 [6] Z. X. Meng, W. Zheng, L. Li, Y. F. Zheng, *Mater. Sci. Eng. C* **30**, 1014 (2010).
- 666 [7] X. Jing, H.-Y. Mi, T. M. Cordie, M. R. Salick, X.-F. Peng, L.-S. Turng, *Polymer* **55**, 5396
667 (2014).
- 668 [8] S. Abbaspoor, S. Agbolaghi, F. Abbasi, *Eur. Polym. J.* **103**, 293(2018).
- 669 [9] C. X. Lam, S. H. Teoh, D. W. Hutmacher, *Polym. Int.* **56**, 718 (2007).
- 670 [10] A. Höglund, M. Hakkarainen, A. Albertsson, *J. Macromol. Sci. Part A* **44**, 1041(2007).
- 671 [11] L. A. Bosworth, S. Downes, *Polym. Degrad. Stab.* **95**, 2269 (2010).
- 672 [12] O. Hartman, C. Zhang, E. L. Adams, M. C. Farach-Carson, N. J. Petrelli, B. D. Chase, J. F.
673 Rabolta, “*Biomaterials* **31**, 5700 (2010).
- 674 [13] J. M. Miszuk, T. Xu, Q. Yao, F. Fang, J. D. Childs, Z. Hong, J. Tao, H. Fong, H. Sun, *Appl.*
675 *Mater. Today* **10**, 194 (2018).
- 676 [14] J. S. Stevens, A. C. de Luca, S. Downes, G. Terenghi, S. L. M. Schroeder, “*Surf. Interface Anal.*,
677 **46**, 673 (2014).
- 678 [15] G. Amokrane, C. Falentin-Daudré, S. Ramtani, V. Migonney, “*IRBM*, **39**, 268–(2018).
- 679 [16] L. A. Can-Herrera, A. Ávila-Ortega, S. de la Rosa-García, A. I. Oliva, J. V. Cauich-Rodríguez,
680 J. M. Cervantes-Uc, “*Eur. Polym. J.* **84**, 502 (2016).

This is the author's peer reviewed, accepted manuscript. However, the online version of record will be different from this version once it has been copyedited and typeset.
PLEASE CITE THIS ARTICLE AS DOI: 10.1116/6.0000429

- 681 [17] M. Asadian, M. Dhaenens, I. Onyshchenko, S. De Waele, H. Declercq, P. Cools, B. Devreese,
682 D. Deforce, R. Morent, N. De Geyter, *ACS Appl. Mater. Interfaces* **10**, 41962 (2018).
- 683 [18] C. Latz, G. Pavon-Djavid, G. Hélarý, M. D. Evans, V. Migonney, *Biomacromolecules* **4**, 766
684 (2003).
- 685 [19] P. Yammine, G. Pavon-Djavid, G. Helary, V. Migonney, *Biomacromolecules* **6**, 2630 (2005).
- 686 [20] F. Anagnostou, A. Debet, G. Pavon-Djavid, Z. Goudaby, G. Hélarý, V. Migonney, *Biomaterials*
687 **27**, 3912 (2006).
- 688 [21] M. Ciobanu, A. Siove, V. Gueguen, L. J. Gamble, D. G. Castner, V. Migonney,
689 *Biomacromolecules* **7**, 755(2006).
- 690 [22] J. Zhou, M. Ciobanu, G. Pavon-Djavid, V. Gueguen, V. Migonney, *Proc. IEEE Engineering in*
691 *Medicine and Biology* **29**, 5115 (2007)
- 692 [23] G. Pavon-Djavid, L. J. Gamble, M. Ciobanu, V. Gueguen, D. G. Castner, V. Migonney,
693 *Biomacromolecules* **8**, 3317 (2007).
- 694 [24] S. Lessim, V. Migonney, P. Thoreux, D. Lutomski, S. Changotade, *Biomed. Mater. Eng.* **4**, 289
695 (2013).
- 696 [25] V.Viateau, J. Zhou, S. Guérard, M. Manassero, M. Thourot, F. Anagnostou, D. Mitton,
697 B.Brulez, V.Migonney, *IRBM* **32**, 118 (2011).
- 698 [26] J. Zhou, M. Manassero, V. Migonney, V. Viateau, *IRBM* **30**, 153 (2009).
- 699 [27] C. Vaquette, V. Viateau, S. Guérard, F. Anagnostou, M. Manassero, D. G. Castner, V.
700 Migonney, *Biomaterials* **34**, 7048 (2013).
- 701 [28] S. Huot, G. Rohman, M. Riffault, A. Pinzano, L. Grossin, V. Migonney, *Biomed. Mater. Eng.*
702 **4**, 281 (2013).
- 703 [29] N. Djaker, S. Brustlein, G. Rohman, S. Huot, M. L. de la Chapelle, V. Migonney, *Biomed. Opt.*
704 *Express* **5**, 149 (2014).
- 705 [30] G. Rohman, S. Huot, M. Vilas-Boas, G. Radu-Bostan, D. G. Castner, V. Migonney, *J. Mater.*
706 *Sci. Mater. Med.* **26**, 5539 (2015).

This is the author's peer reviewed, accepted manuscript. However, the online version of record will be different from this version once it has been copyedited and typeset.
PLEASE CITE THIS ARTICLE AS DOI: 10.1116/6.0000429

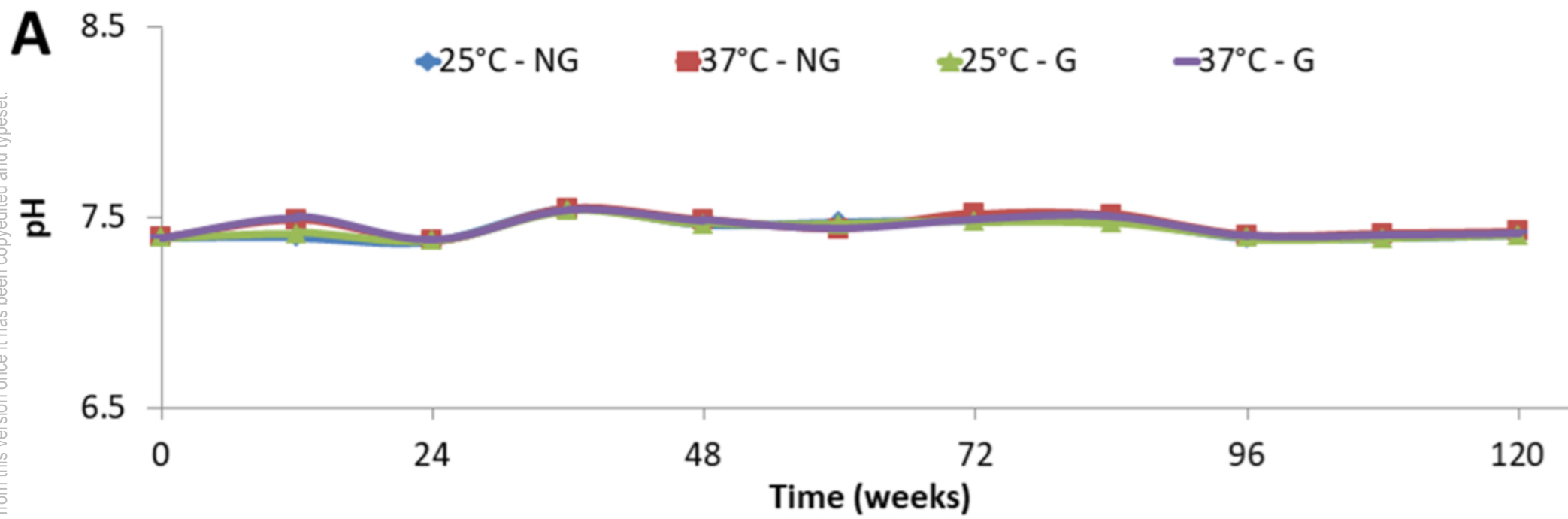
- 707 [31] A. Leroux, C. Egles, V. Migonney, *PloSone* **13**, 205722 (2018).
- 708 [32] A. Leroux, E. Maurice, V. Viateau, V. Migonney, *IRBM*, **40**, 38 (2019).
- 709 [33] M. A. Woodruff, D. W. Hutmacher, *Prog. Polym. Sci.* **35**, 1217 (2010).
- 710 [34] T. Ivanova, N. Grozev, I. Panaiotov, J. E. Proust, “*Colloid Polym. Sci.* **277**, 709 (1999).
- 711 [35] Sandra Sánchez-González, Nazely Diban, Ane Urtiaga, *Membranes*, **8**, 12, (2018).
- 712 [36] C. X. F. Lam, M. M. Savalani, S.-H. Teoh, D. W. Hutmacher, “*Biomed. Mater.* **3**, 034108
- 713 (2008).
- 714 [37] H.-J. Sung, C. Meredith, C. Johnson, Z. S. Galis, *Biomaterials* **25**, 5735 (2004).
- 715 [38] A.C. Vieira, J.C. Vieira, J.M. Ferra, F.D. Magalhães, R.M. Guedes, A.T. Marques. *J. Mech.*
- 716 *Behav. Biomed. Mater.* **4**, 451(2011).
- 717 [39] I. Castilla-Cortázar, J. Más-Estellés, J. M. Meseguer-Dueñas, J. L. Escobar Ivirico, B. Marí, A.
- 718 Vidaurre, *Polym. Degrad. Stab.* **97**, 1241(2012).
- 719 [40] D. C. França, E. B. Bezerra, D. D. de S. Morais, E. M. Araújo, R. M. R. Wellen, *Mater. Res.*,
- 720 **19**, 618 (2016).
- 721 [41] G. P. Sailema-Palate, A. Vidaurre, A. J. Campillo-Fernández, I. Castilla-Cortázar, *Polym.*
- 722 *Degrad. Stab.* **130**, 118 (2016).
- 723 [42] D. C. França, D. D. Morais, E. B. Bezerra, E. M. Araújo, R. M. R. Wellen, *Mater. Res.* **21**, 5,
- 724 (2018).
- 725 [43] H. Samami, J. Pan, *J. Mech. Behav. Biomed. Mater.* **59**, 430 (2016).
- 726 [44] K. Sevim, J. Pan, *Acta Biomater.* **66**, 192 (2018).
- 727 [45] Q. Zhang, Y. Jiang, Y. Zhang, Z. Ye, W. Tan, M. Lang, *Polym. Degrad. Stab.* **98**, 209 (2013).
- 728 [46] G. Liao, S. Jiang, X. Xu, Y. Ke, *Mater. Lett.* **82**, 159 (2012).
- 729 [47] P. S. P. Poh, D. W. Hutmacher, B. M. Holzapfel, A. K. Solanki, M. A. Woodruff, *Data Brief* **7**,
- 730 923 (2016).
- 731 [48] Y. Shi, J. Liu, L. Yu, L. Z. Zhong, H. B. Jiang, *Ceram. Int.* **44**, 15086 (2018).
- 732 [49] M. Marrese, V. Cirillo, V. Guarino, L. Ambrosio, *J. Funct. Biomater.* **9**, 27 (2018).

This is the author's peer reviewed, accepted manuscript. However, the online version of record will be different from this version once it has been copyedited and typeset.
PLEASE CITE THIS ARTICLE AS DOI: 10.1116/6.0000429

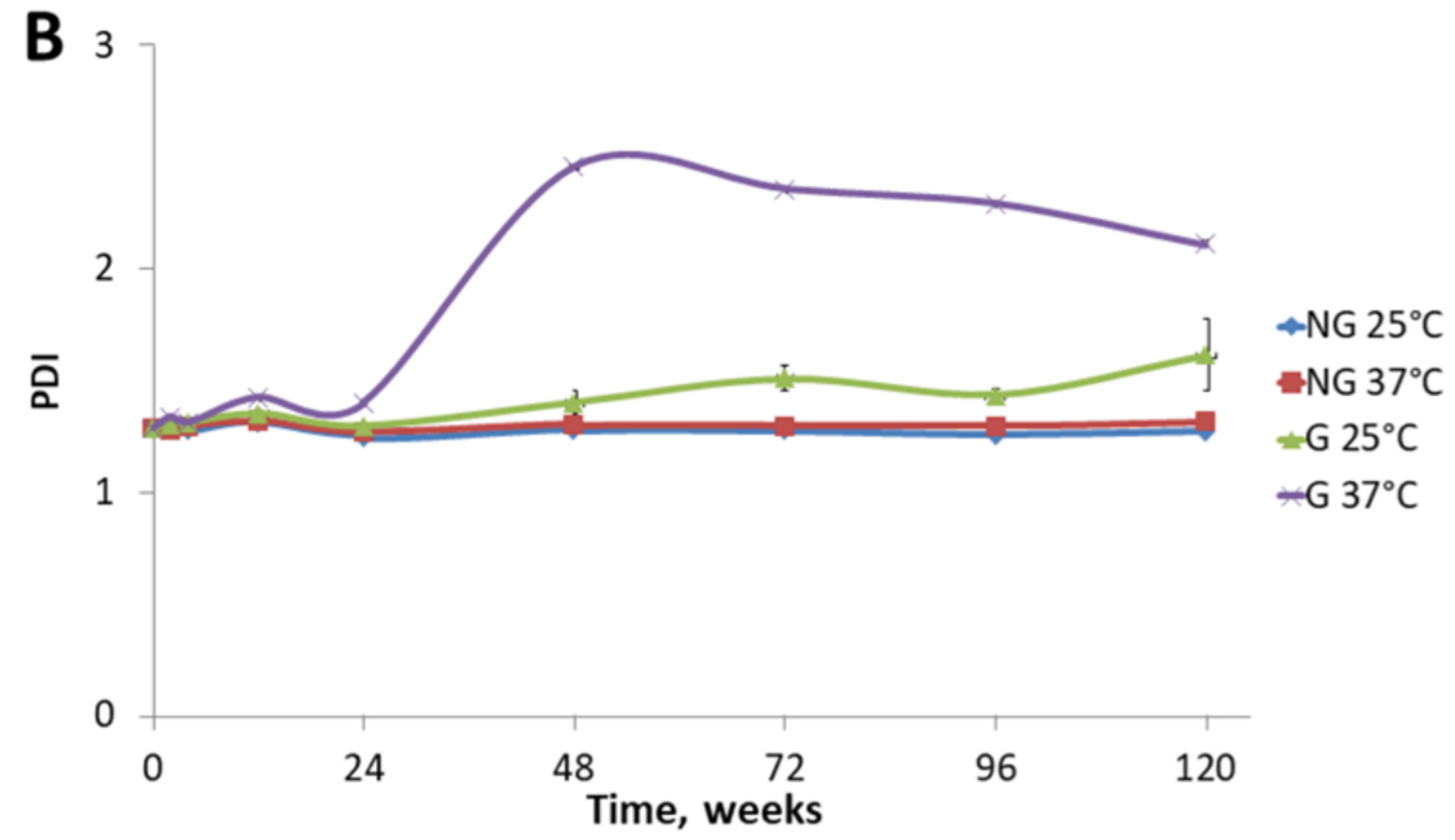
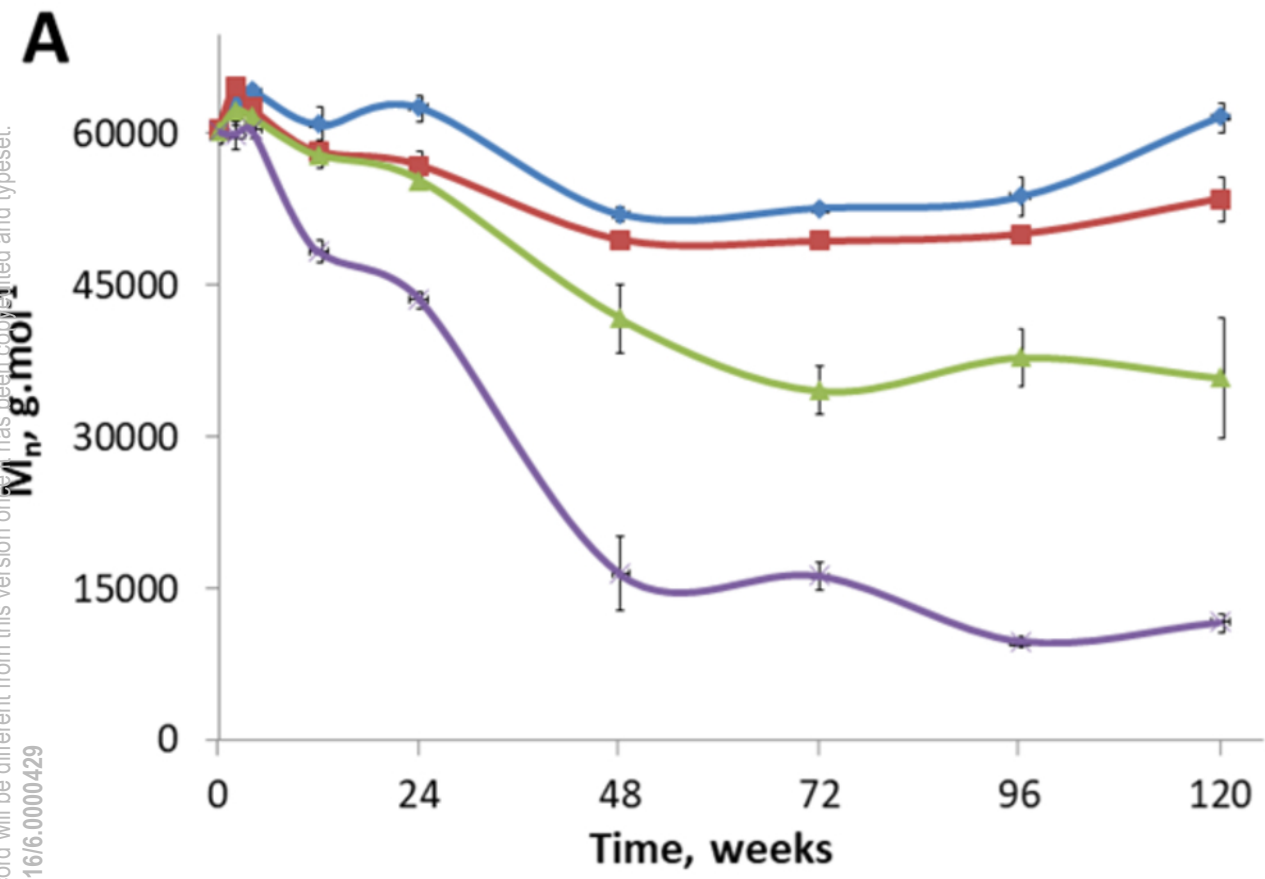
- 733 [50] M. A. Basile, G. G. d'Ayala, M. Malinconico, P. Laurienzo, J. Coudane, B. Nottelet, F.
734 DellaRagione, A. Oliva, *Mater. Sci. Eng. C* **48**, 457 (2015).
- 735 [51] L. Ghasemi-Mobarakeh, M. P. Prabhakaran, M. Morshed, M. H. Nasr-Esfahani, S.
736 Ramakrishna, "*Mater. Sci. Eng. C* **30**, 1129 (2010).
- 737 [52] H. Y. Kweon, M. K. Yoo, I. K. Park, T. H. Kim, H. C. Lee, H. Lee, J. Oh, T. Akaike, C. Cho
738 *Biomaterials* **24**,801(2003).
- 739 [53] L. Goebel, P. Orth, M. Cucchiarini, D. Pape, H. Madry, *Osteoarthritis Cartilage* **25**, 581 (2017).
- 740 [54] K. J. Livak, T. D. Schmittgen, *Methods* **25**, 402 (2001).
- 741 [55] B. Nie, J. Stutzman, A. Xie, *Biophys. J.* **88**, 2833(2005).
- 742 [56] A. Rangel, L. Colaço, N.T. Nguyen, J.-F. Grosset, C. Egles, V. Migonney, *IRBM*,
743 <https://doi.org/10.1016/j.irbm.2020.10.002>. 2020.
- 744 [57] S. C. Woodward, P. S. Brewer, F. Moatamed, A. Schindler, C. G. Pitt, *J. Biomed. Mater. Res.*,
745 **19**, 437 (1985).
- 746 [58] D. D. Deligianni, N. Katsala, S. Ladas, D. Sotiropoulou, J. Amedee, Y. F. Missirlis,
747 *Biomaterials* **22**, 1241(2001).
- 748 [59] E. Rosqvist, E. Niemelä, A. P. Venu, R. Kummala, P. Ihalainen, M. Toivakka, J. E. Eriksson, J.
749 Peltonen, *Colloids Surf. B Biointerfaces* **174**, 136 (2019).
- 750 [60] C. G. Pitt, F. I. Chasalow, Y. M. Hibionada, D. M. Klimas, A. Schindler, *J. Appl. Polym. Sci.*
751 **26**, 3779 (1981).
- 752 [61] T. Sekiguchi, A. Saika, K. Nomura, T. Watanabe, T; Watanabe, Y. Fujimoto, M. Enoki, T. Sato,
753 C. Kato, H. Kanehiro, *Polym. Degrad. Stab.* **96**, 1397 (2011).
- 754

This is the author's peer reviewed, accepted manuscript. However, the online version of record will be different from this version once it has been copyedited and typeset.

PLEASE CITE THIS ARTICLE AS DOI: 10.1116/6.0000429

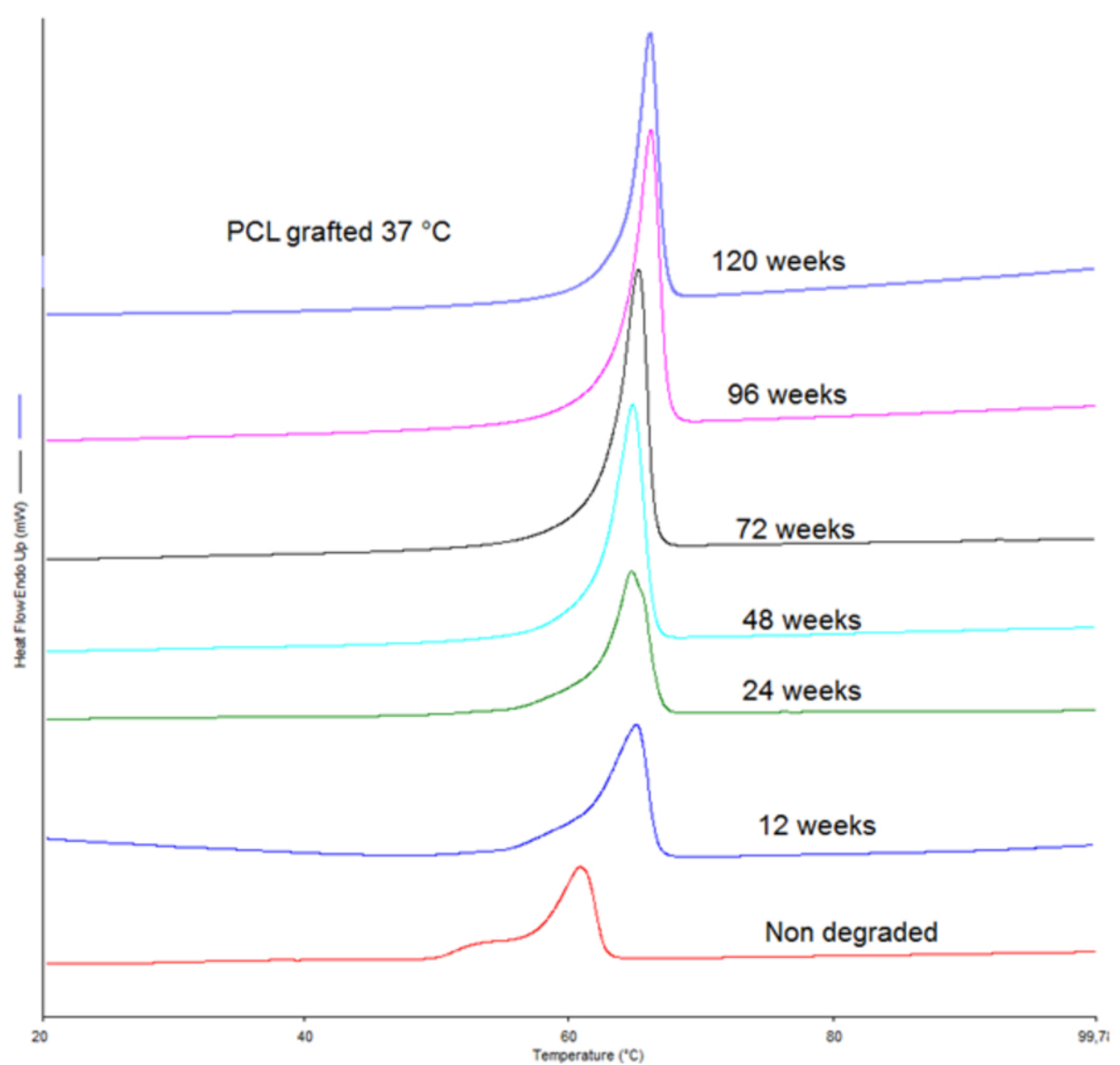
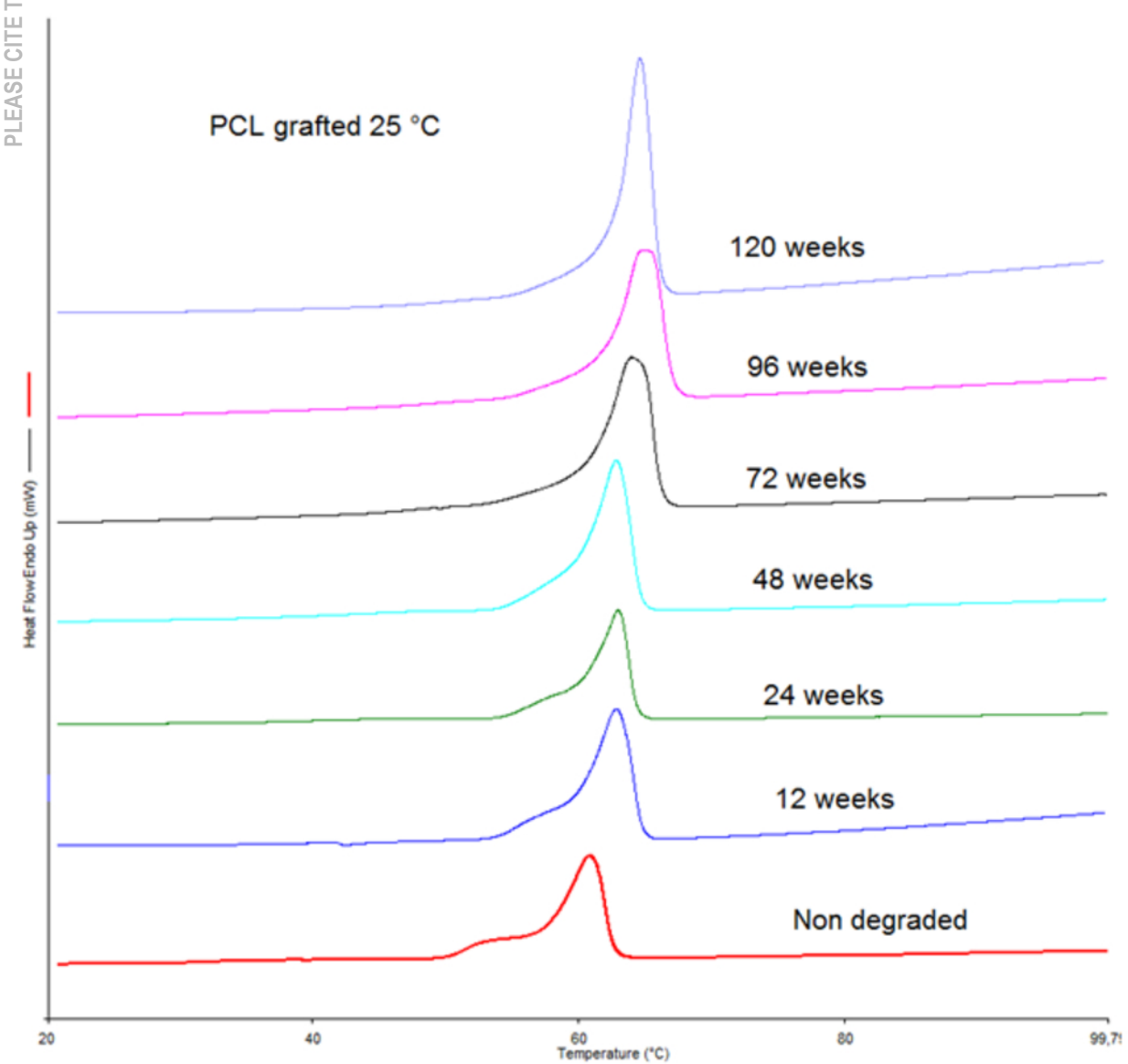
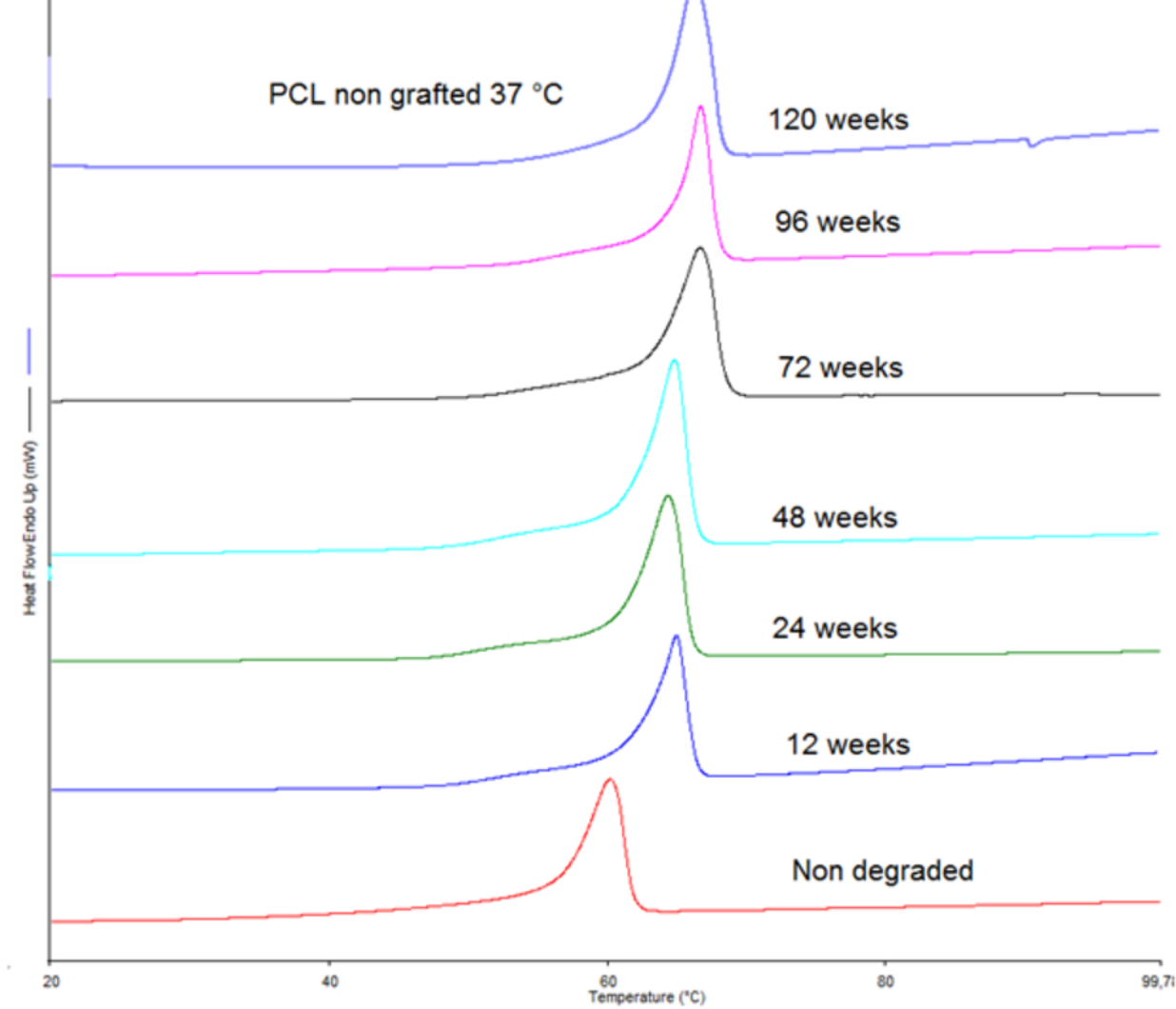
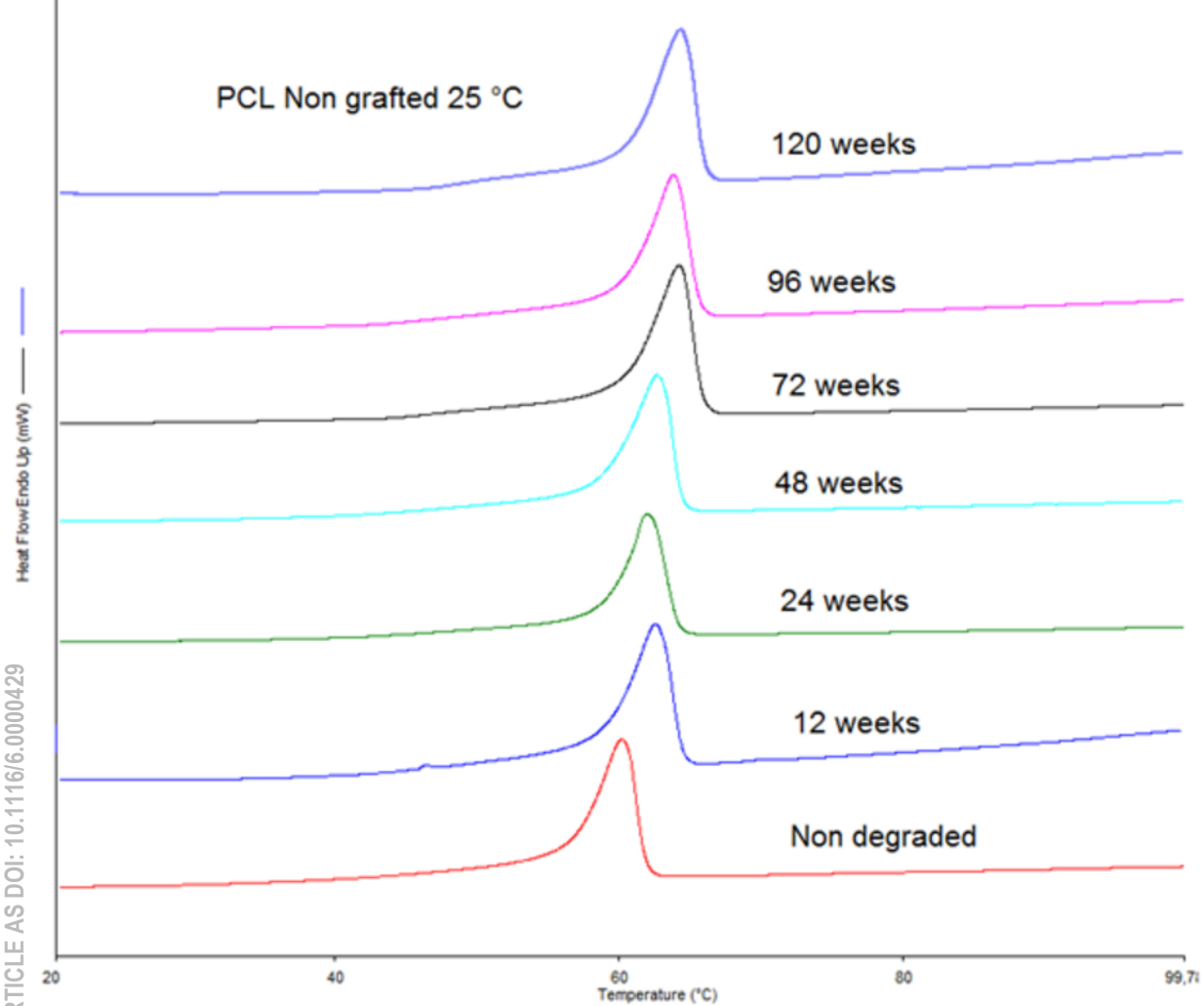


This is the author's peer reviewed, accepted manuscript. However, the online version of record will be different from this version once it has been copyedited and typeset.
PLEASE CITE THIS ARTICLE AS DOI: 10.1116/6.0000429

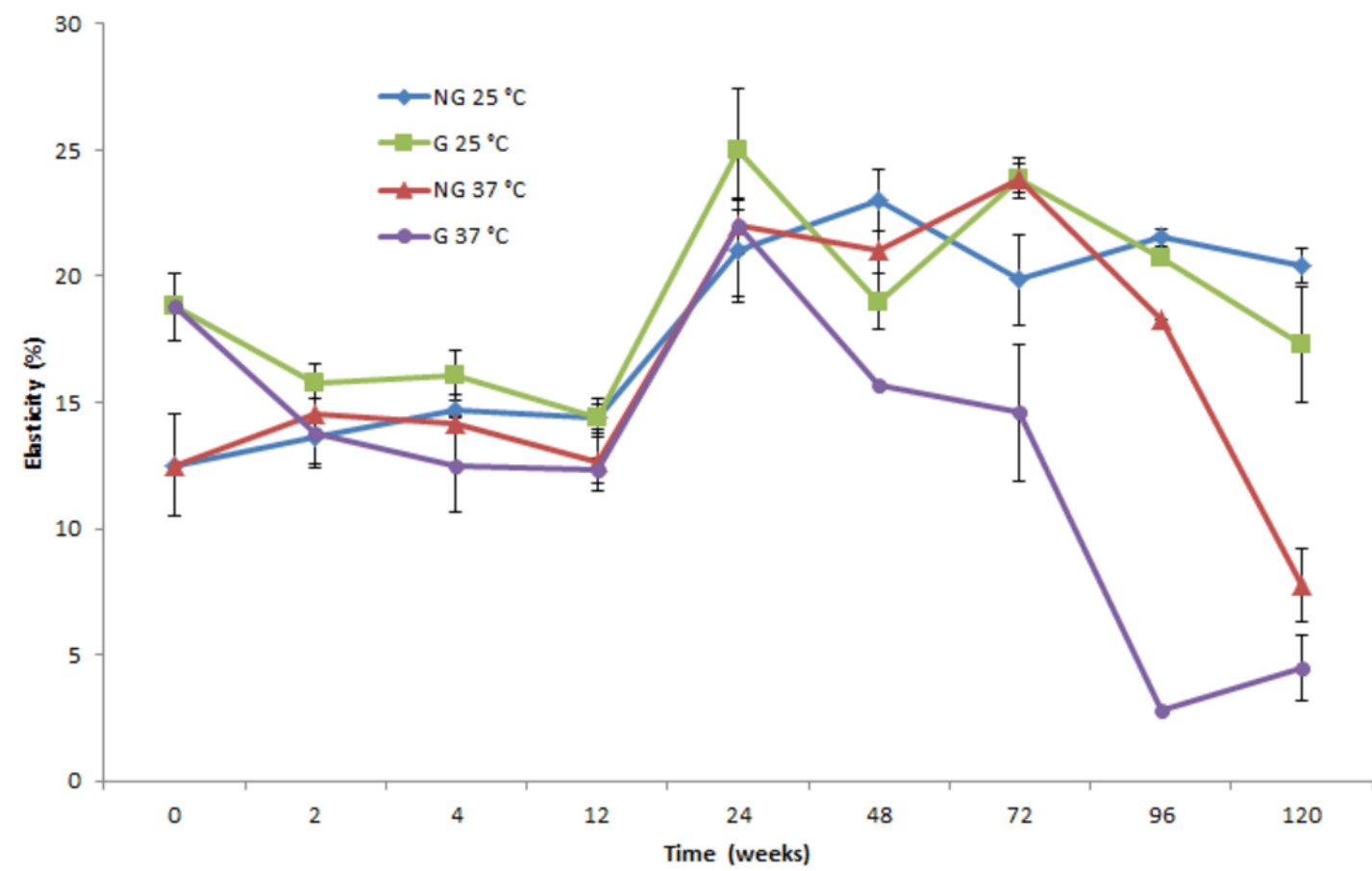
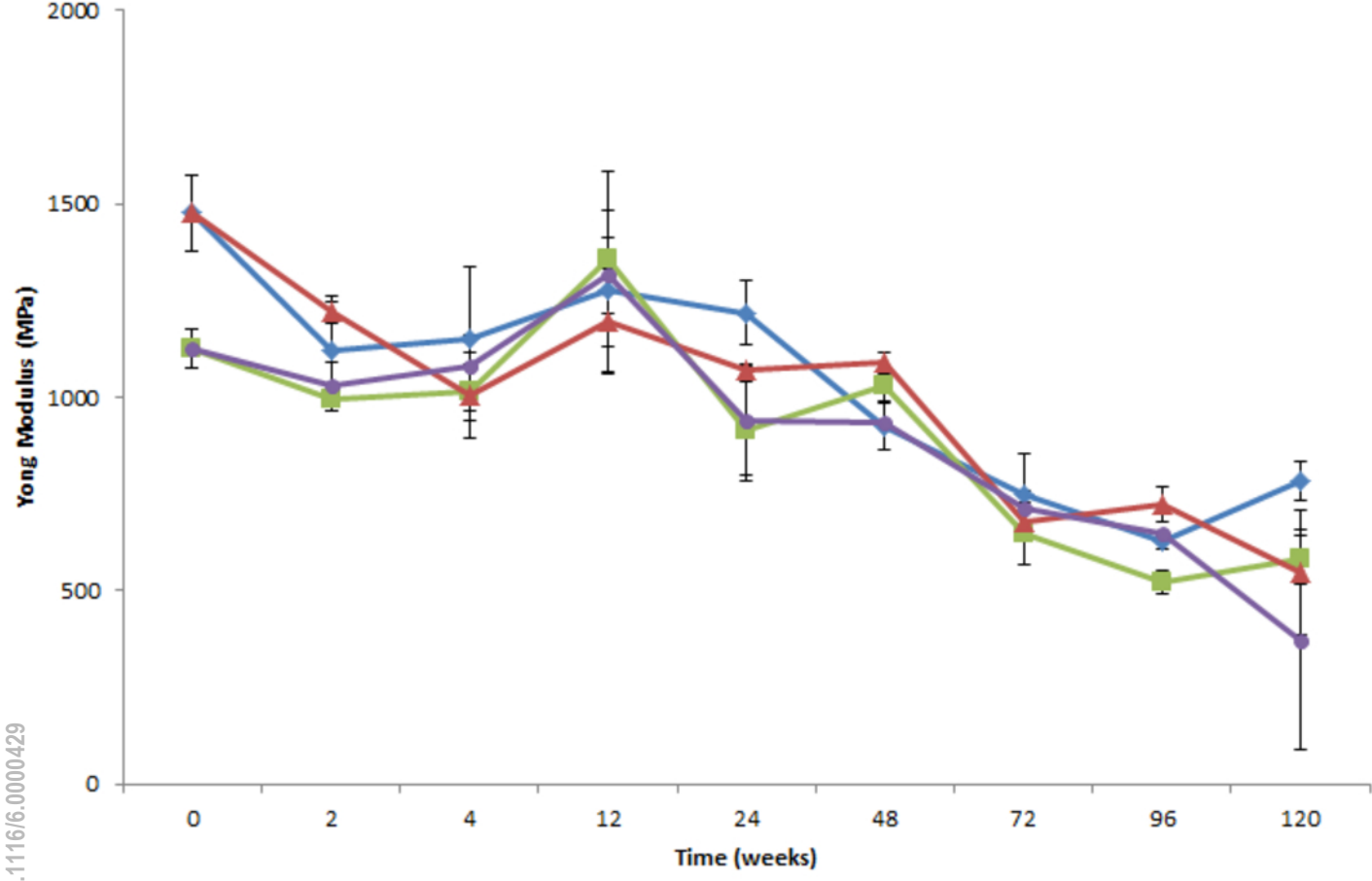




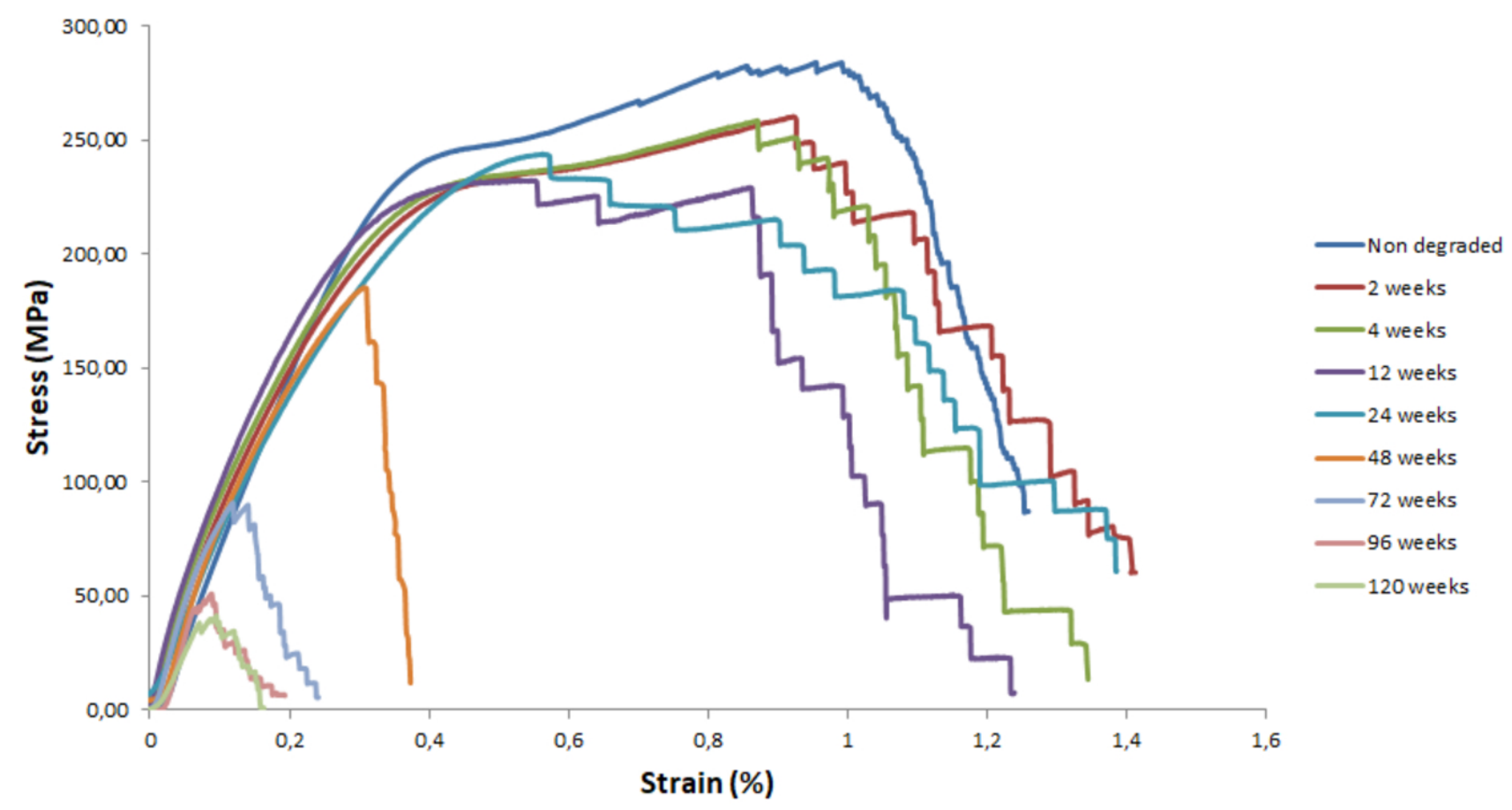
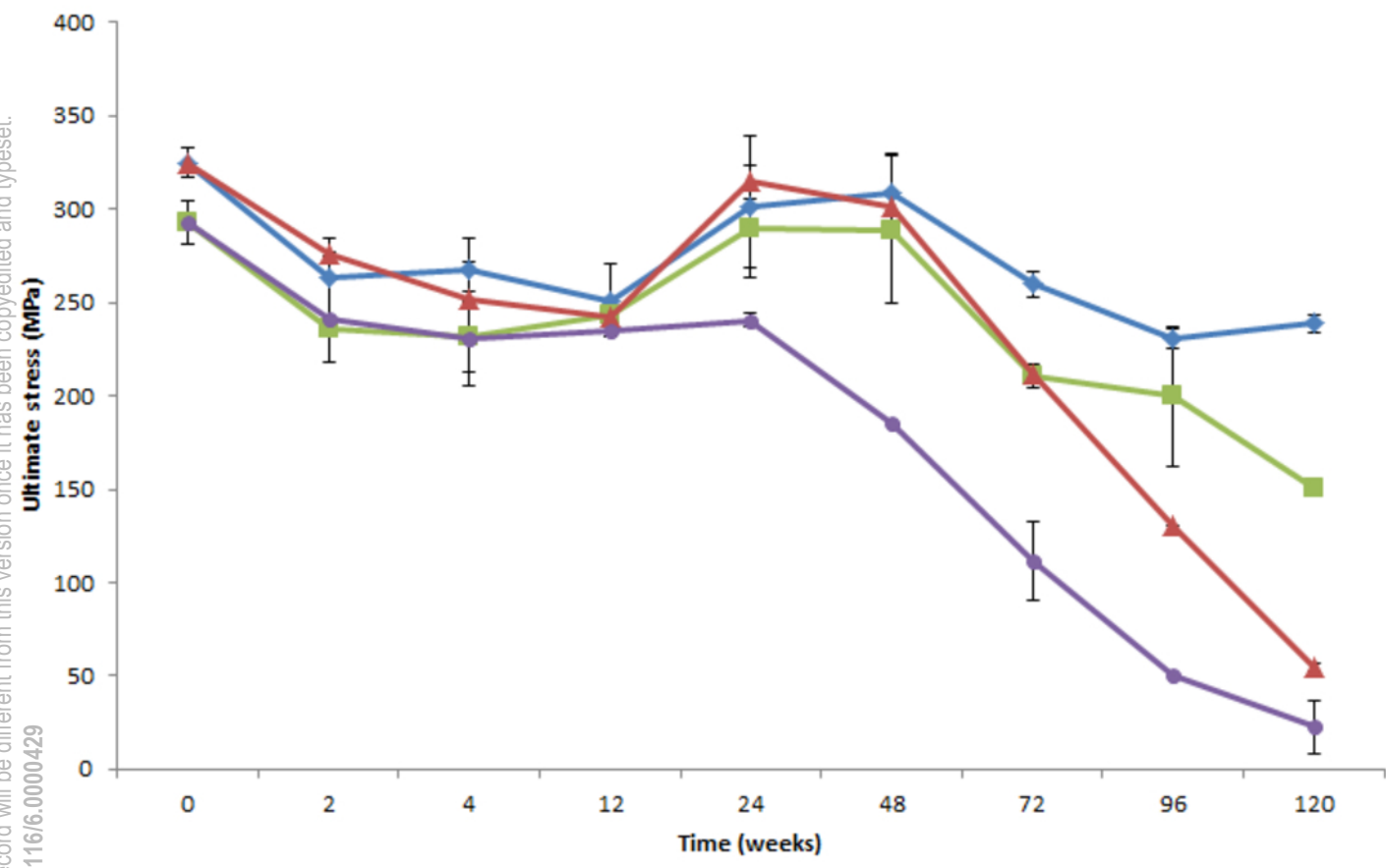
This is the author's peer reviewed, accepted manuscript. However, the online version of record will be different from this version once it has been copyedited and typeset.
PLEASE CITE THIS ARTICLE AS DOI: 10.1116/6.0000429



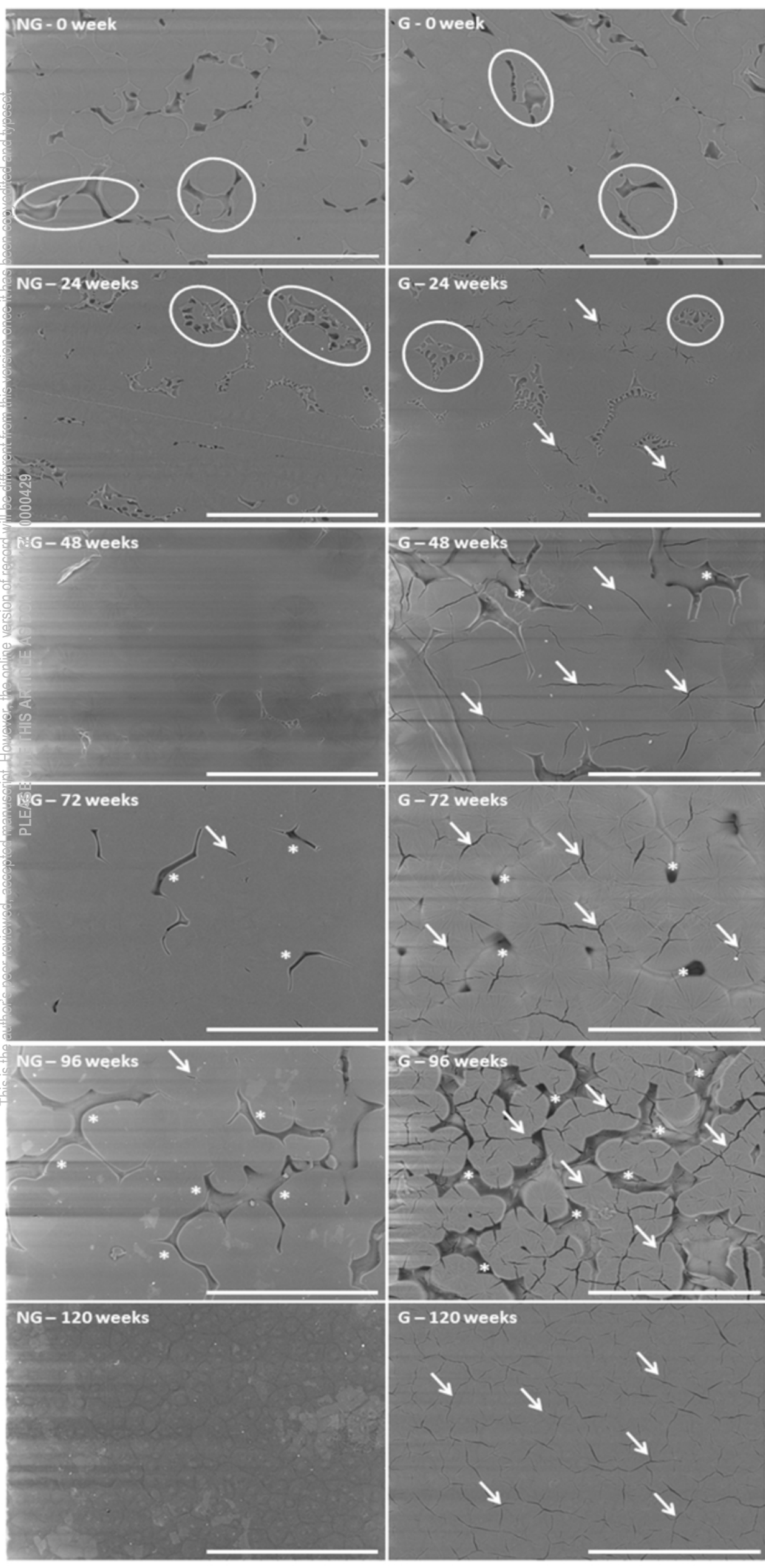
This is the author's peer reviewed, accepted manuscript. However, the online version of record will be different from this version once it has been copyedited and typeset.
 PLEASE CITE THIS ARTICLE AS DOI: 10.1116/16.0000429



This is the author's peer reviewed, accepted manuscript. However, the online version of record will be different from this version once it has been copyedited and typeset.
PLEASE CITE THIS ARTICLE AS DOI: 10.1111/6.0000429

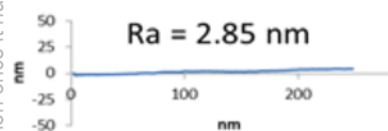
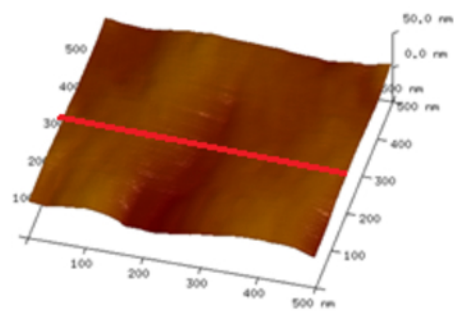


This is the author's peer-reviewed, accepted manuscript. However, the online version of record will be different from this version once it has been copy-edited and typeset. PLEASE CHECK THIS ARTICLE AGAINST THE PROOF. 0000429

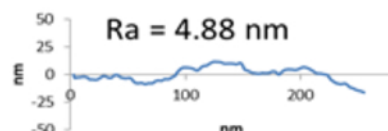
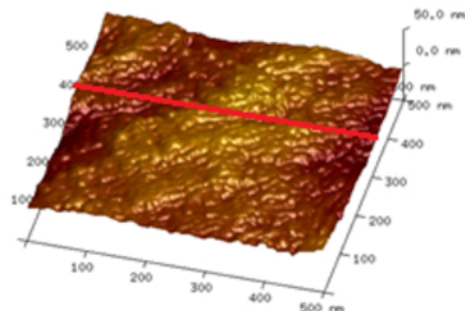


This is the author's peer reviewed, accepted manuscript. However, the online version of record will be different from this version once it has been copyedited and typeset.
PLEASE CITE THIS ARTICLE AS DOI: 10.1116/6.0000429

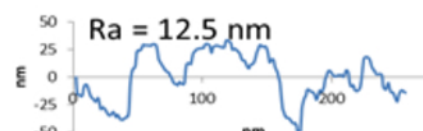
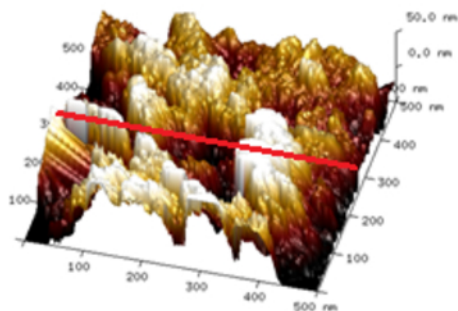
(a) Film NG-0 w



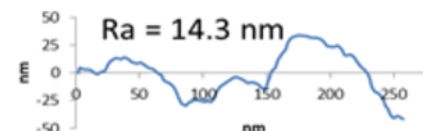
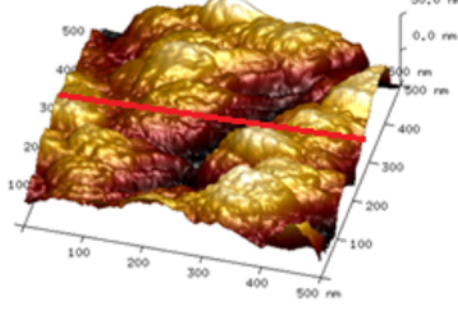
(b) Film NG-24 w



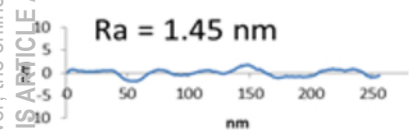
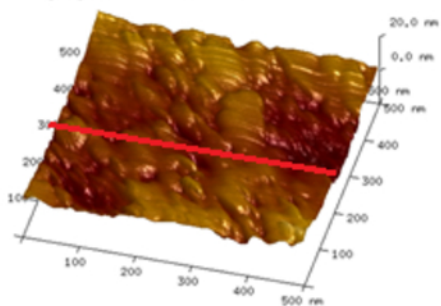
(c) Film NG-96 w



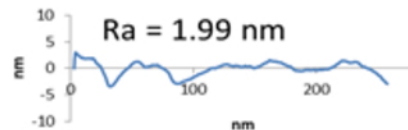
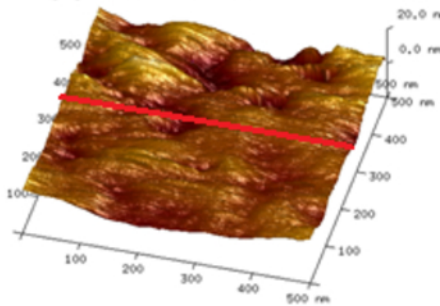
(d) Film NG-120 w



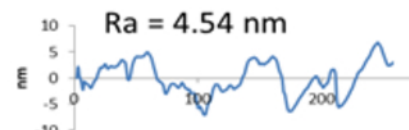
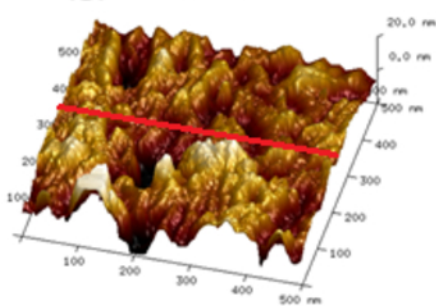
(e) Film G-0 w



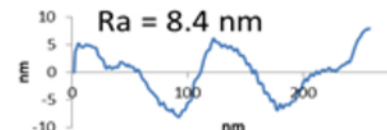
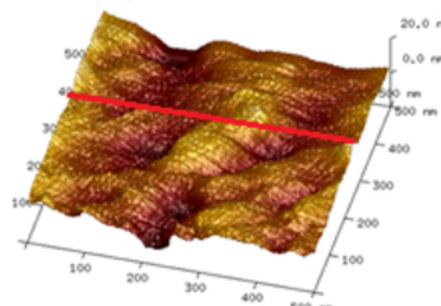
(f) Film G-24 w



(g) Film G-96 w



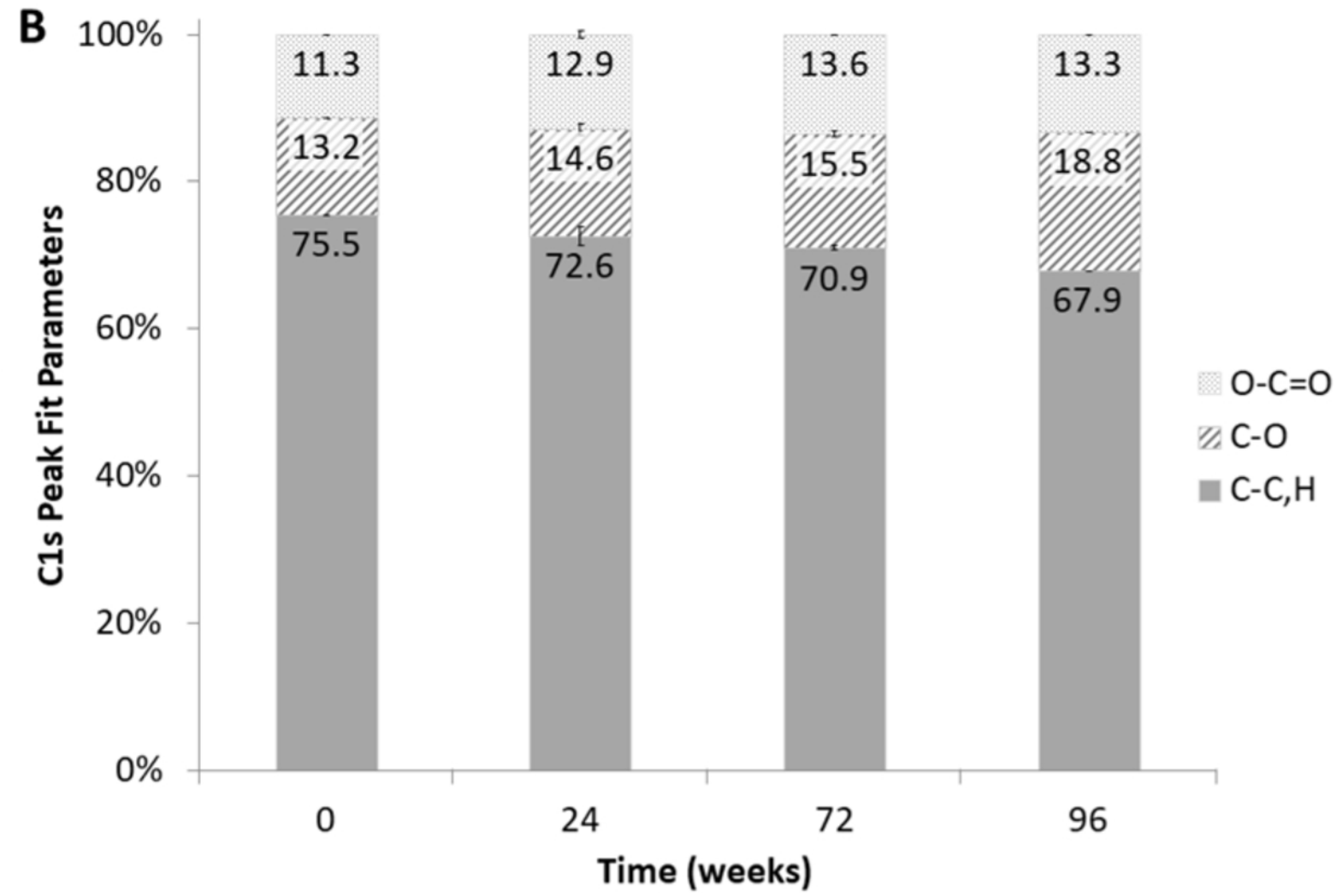
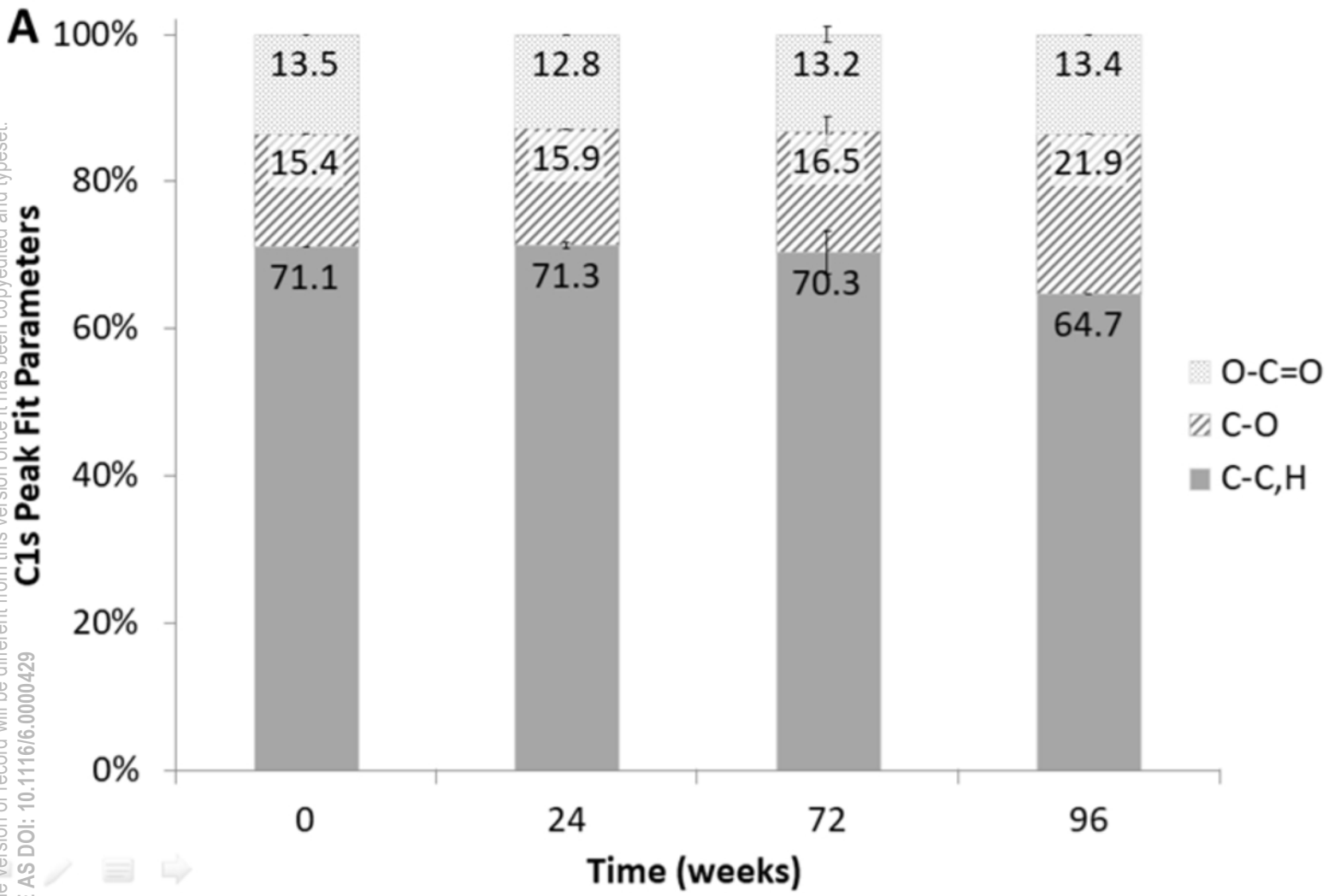
(h) Film G-120 w



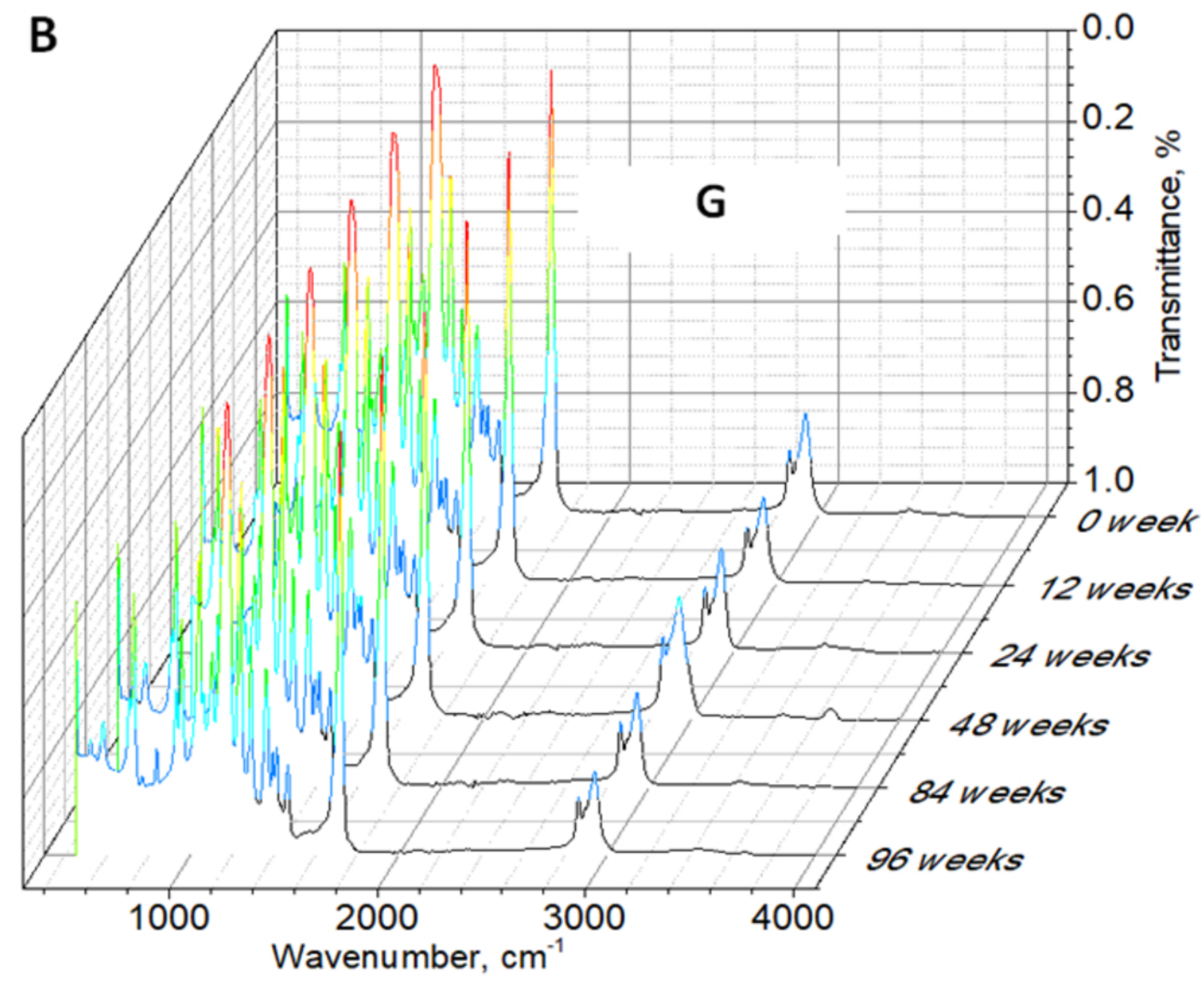
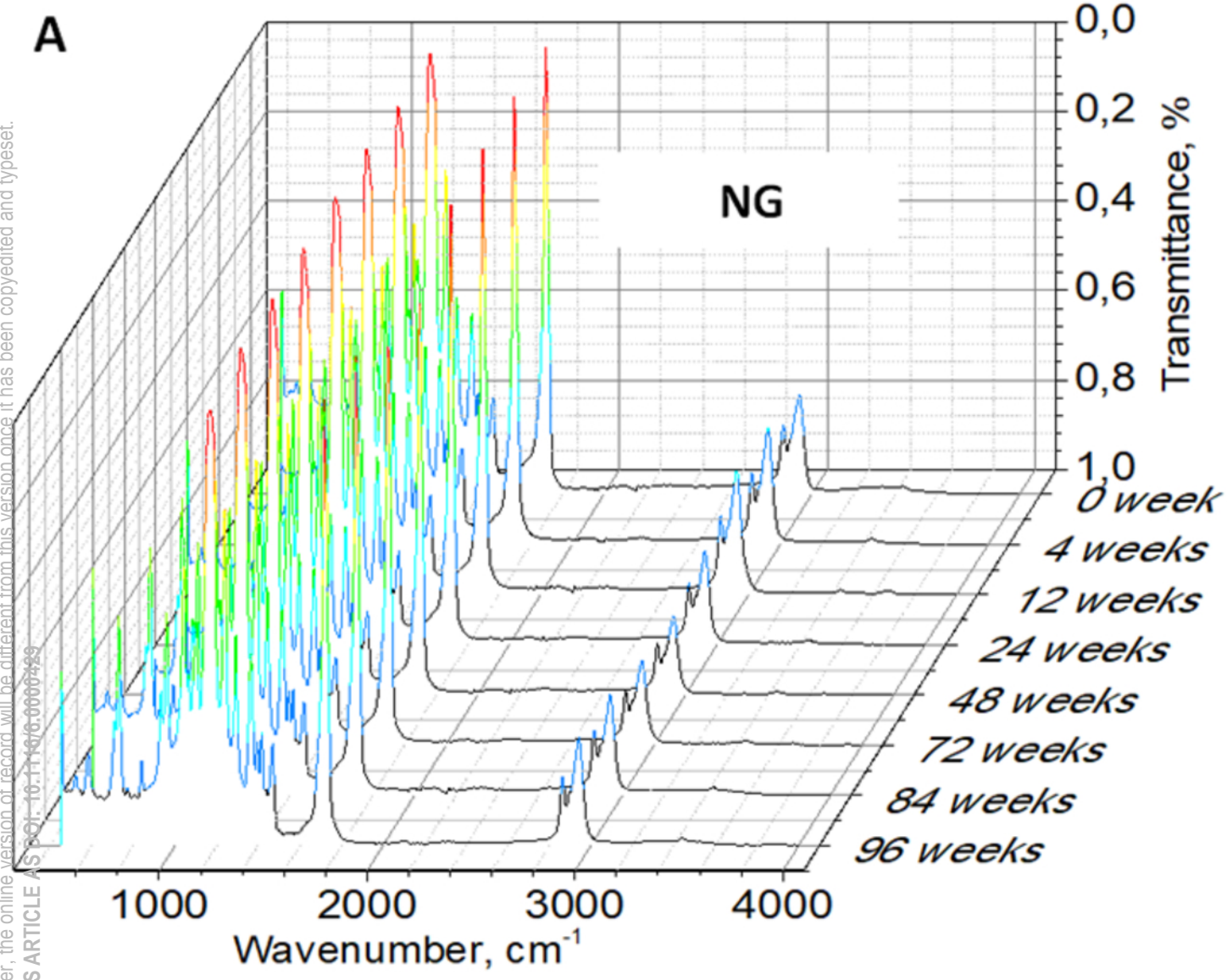
This is the author's peer reviewed, accepted manuscript. However, the online version of record will be different from this version once it has been copyedited and typeset.

PLEASE CITE THIS ARTICLE AS DOI: 10.1116/6.0000429

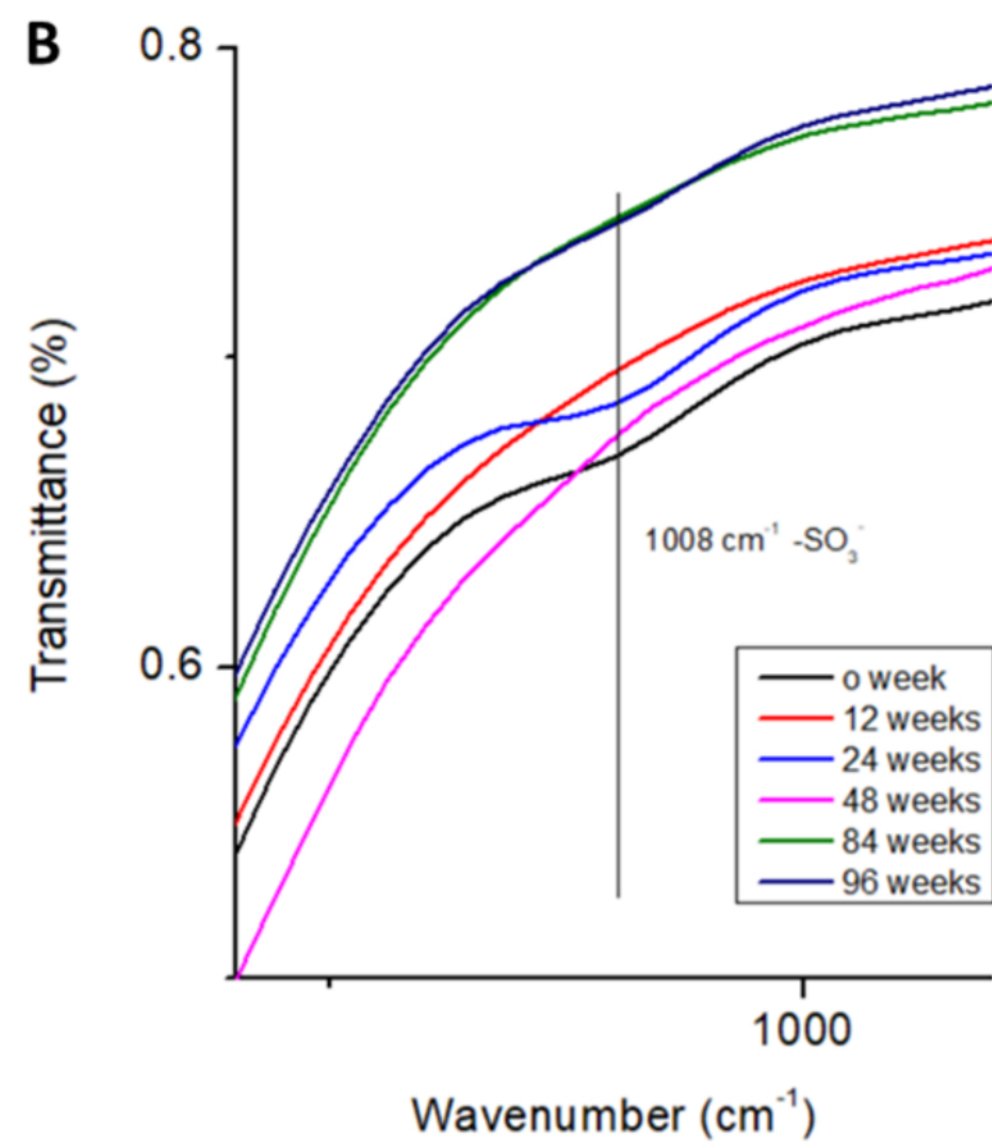
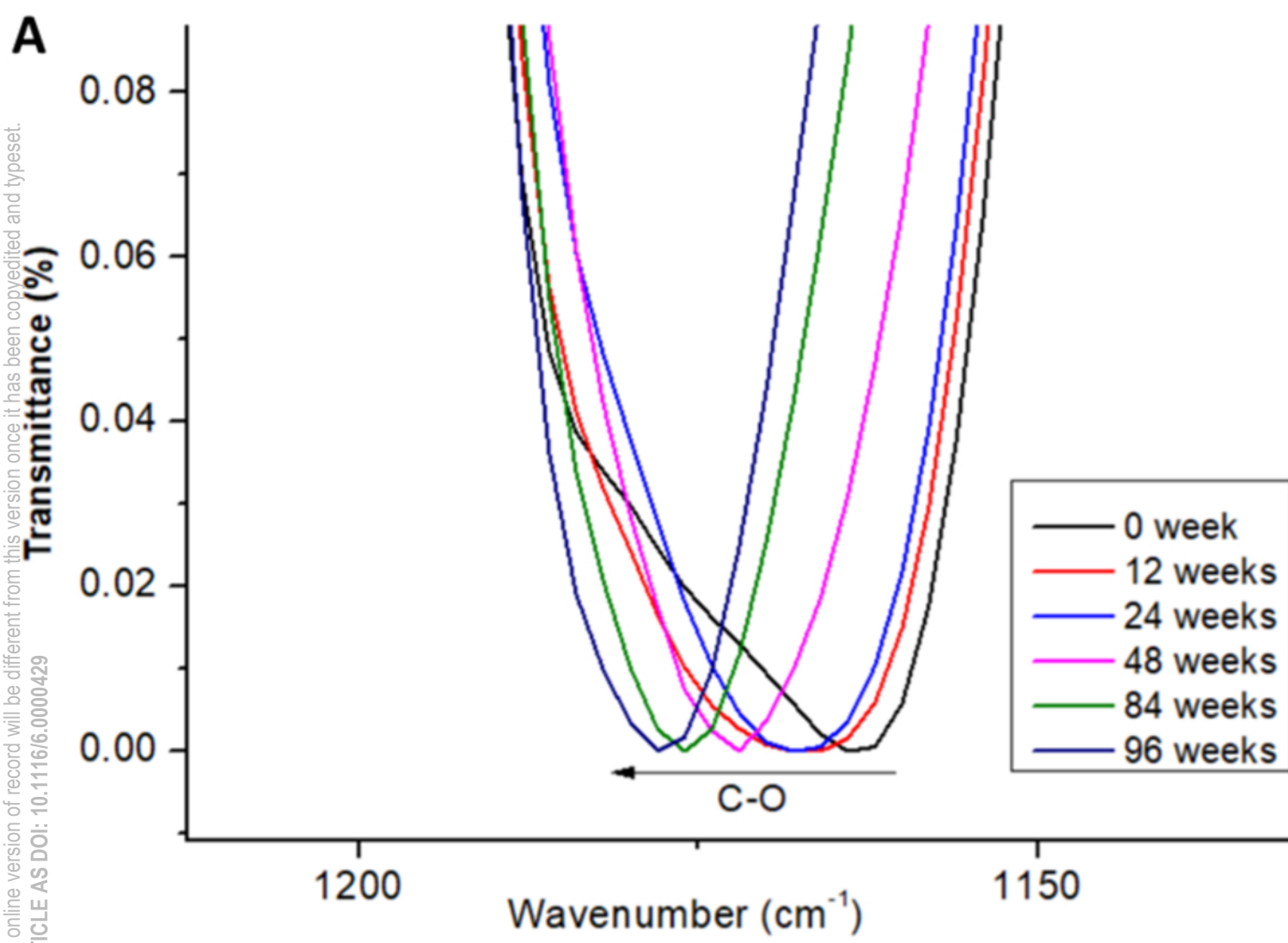
C1s Peak Fit Parameters



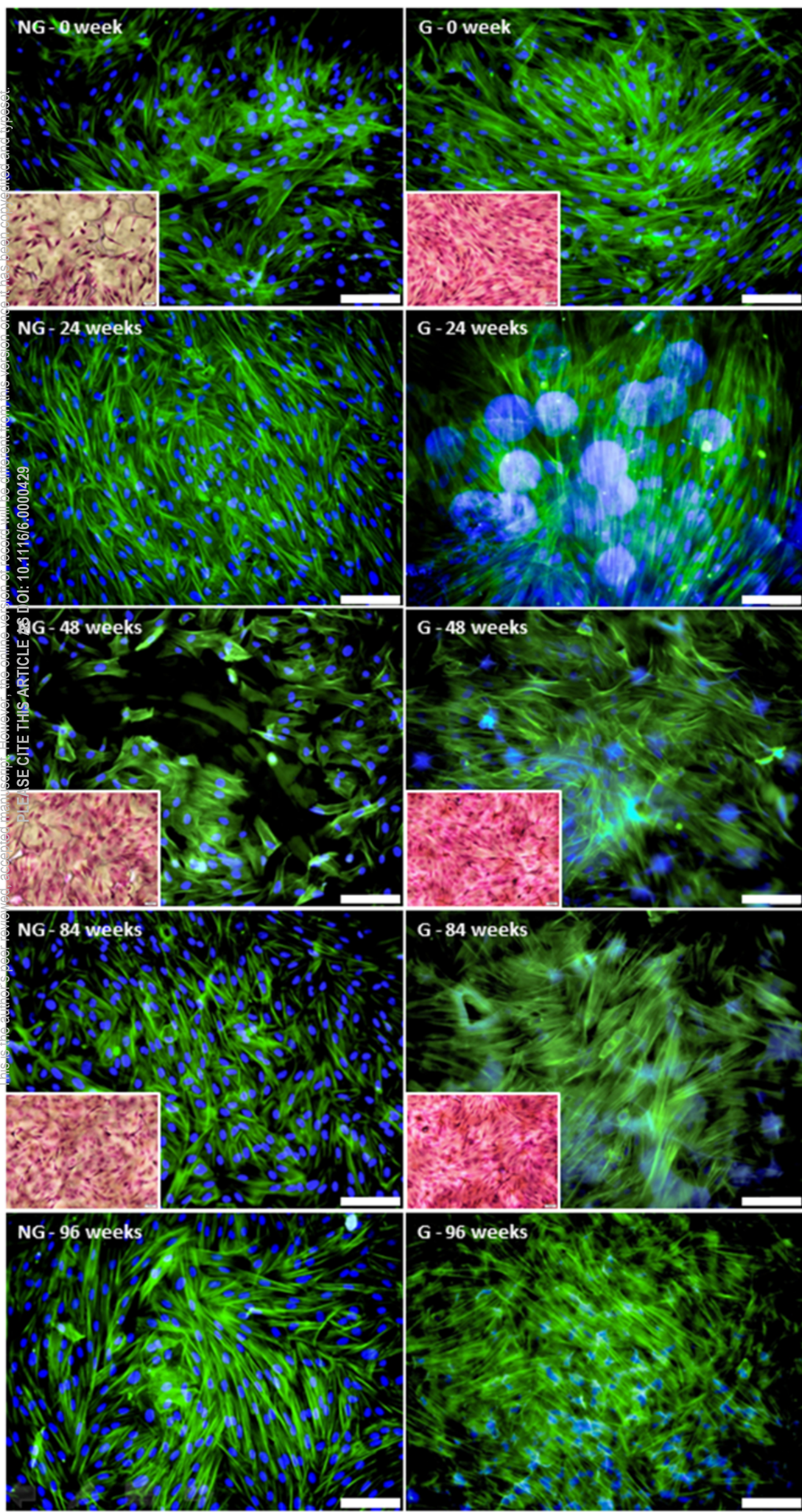
This is the author's peer reviewed, accepted manuscript. However, the online version of record will be different from this version once it has been copyedited and typeset.
PLEASE CITE THIS ARTICLE AS DOI: 10.1116/1.5000000



This is the author's peer reviewed, accepted manuscript. However, the online version of record will be different from this version once it has been copyedited and typeset.
PLEASE CITE THIS ARTICLE AS DOI: 10.1116/6.0000429



This is the author's peer-reviewed, accepted manuscript. However, the online version of record will be different from this version once it has been copyedited and typeset. PLEASE CITE THIS ARTICLE AS DOI: 10.1116/6.0000429



This is the author's peer reviewed, accepted manuscript. However, the online version of record will be different from this version once it has been copyedited and typeset.
PLEASE CITE THIS ARTICLE AS DOI: 10.1116/6.0000429

